ORAL DISEASES
Leading in Oral, Maxillofacial, Head & Neck Medicine

Oral Diseases (2016) 22, 247–248 doi:10.1111/odi.12445

www.wiley.com

INVITED COMMENTARY

On the origin of blood cells – hematopoiesis revisited

Éva Mezey
Adult Stem Cell Section, CSDB, NIDCR, NIH, Bethesda, MD, USA

Faiyaz Notta and his colleagues from Dr. John Dick's group in Canada recently published an elegant study of blood cell development in Science (Notta *et al*, 2015). Their data suggest that a different model from the prevailing one may explain the origin of diverse cells found in blood. This involves hematopoiesis, a term derived from two Greek words: *haima* (blood) and *poiēsis* (to produce something). The process occurs in bone marrow (BM) and other organs: liver and umbilical cord in the fetus, and spleen in species like mice. In BM, hematopoietic stem cells (HSCs) give rise to all blood cell lineages (Ogawa, 1993; Al-Drees *et al*, 2015; Barminko *et al*, 2015).

The formation of blood cells from HSCs moves through a series of more and more differentiated (and 'committed') progenitor cells – a hematopoietic hierarchy (Ackermann *et al*, 2015). An excellent review of the history of the discovery of blood stem cells was written by Ramalho-Santos and Willenbring (Ramalho-Santos and Willenbring, 2007). A brief summary follows:

In the early 1960s, Till and McCulloch showed that there is a population of BM cells in animals that can repopulate the BM if one destroys it with lethal irradiation, for example (Till *et al*, 1964). Subsequently, it was discovered that such stem cells circulate in the blood too, and in the 1990s, methods were developed that allowed these cells to be purified so that they could be transplanted into human patients (Bensinger *et al*, 1996; Shpall *et al*, 1999). The technique relied on boosting stem cell numbers in the blood of donors by treating them with cytokines that drive the exit of progenitors from BM and their entry into blood. The discovery, characterization, and use of multipotent stem cells that can give rise to a variety of blood cells have allowed previously fatal diseases to be treated.

Characterization of stem- and progenitor cells in BM has relied on specific surface markers that allow subpopulations of cells to be isolated using fluorescence-activated cell sorting (FACS; Akashi *et al*, 2000; Kondo *et al*, 1997). *In vitro* assays (colony-forming unit or CFU assays) are used to learn what kinds of cells the isolated progenitors produce. Such assays have revealed the lineage potential of progenitors in defined environments. (cytokines and growth factors affect the outcome of such analyses.) It is thought that subsets of BM cells isolated by FACS using antibodies directed against specific sets of surface markers are functionally homogeneous (Manz *et al*, 2002), and based on this, a cellular hierarchy, which is pyramidal in shape, has been suggested to account for the development and expansion of blood cell lineages (Figure 1a). According to this model, oligopotent HSCs that spawn all blood cell types differentiate into a variety of multipotent progenitors that are capable of giving rise to several, but not all, of these blood cells. Multipotent progenitors, in turn, generate unipotent cells that can only differentiate into a single blood cell lineage. Although several groups have questioned specific details of the model outlined above (Adolfsson *et al*, 2005; Mansson *et al*, 2007), no one until now has tried to re-evaluate (and re-imagine) the whole process. This is what Notta and his

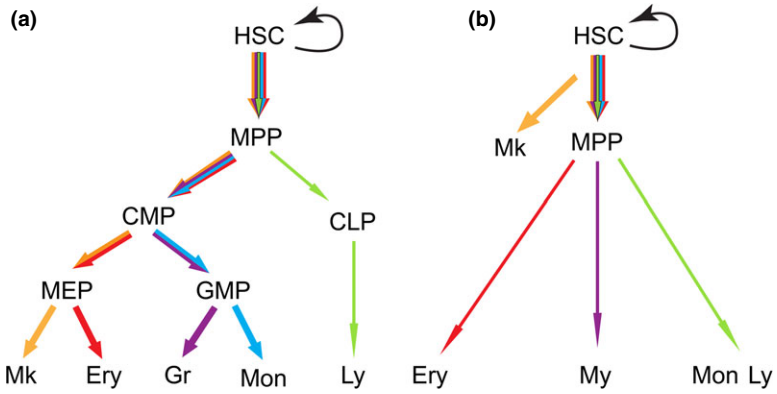

Figure 1 (**a**) Conventional depiction of human hematopoiesis. The oligopotent hematopoietic stem cell (HSC) is at the top of the pyramid. (This cell can reproduce itself and differentiate into all lineages.) MPP cells are multipotent progenitors with limited self-renewal and multilineage reconstitution capacity. They give rise to the common myeloid progenitor (CMP) and the common lymphoid progenitor (CLP) that generates lymphocytes (Ly). CMPs differentiate into megakaryocyte (Mk)/erythroid (Ery) progenitor cells (MEPs) and granulocyte (Gr)/monocyte (Mon) progenitors (GMP). According to this hypothesis, multipotent, oligopotent and then lineage-restricted cells are derived gradually, one after another, from HSCs. (**b**) New hypothesis of human adult hematopoiesis. The oligopotent HSC first gives rise to the Mk lineage and multipotent MPP cells. The latter give rise to three unipotent lineages: the erythroid (Ery), myeloid (My) and the monocytic/lymphoid (Mono-Ly) lineages

colleagues set out to do. They obtained samples of fetal liver, umbilical cord blood, and BM aspirates from normal subjects and patients with aplastic anemia and developed a novel cell sorting method that appears to resolve myeloid, erythroid, and megakaryocytic lineages produced from single CD34+ progenitor cells. They went on to create an assay that allowed them to evaluate the lineage potential of single sorted cells, and an expression profiling technique that could be applied to thousands of HSCs and progenitors isolated from cord blood.

Based on the work they did, they concluded that (1) the cellular hierarchy of human blood elements changes during development, and (2) in contrast to the present view, there are no intermediate oligopotent progenitors. Instead, after the megakaryocytic lineage branches off, three unilineage progenitors are left. These give rise to erythroid, myeloid, and lymphoid cells, respectively (Figure 1b).

If these findings are confirmed, BM stem cell populations must be much more heterogeneous than we thought they were, and we will have to account for the newly revealed complexity. We will also have to review data in the literature to see whether we need to revise our interpretation of them based on this newly discovered hierarchy of blood progenitors.

Significance of the finding:

- Notta's data should contribute to a better understanding of hematological diseases – genetic and/or epigenetic ones.
- A more accurate description of blood cell lineages should help scientists isolate cells that can be used in regenerative medicine using IPS (induced pluripotent stem cell) technology (Yamanaka, 2007). We should soon be able to manufacture red blood cells and platelets that can be given to patients who are deficient in these blood elements, and identifying the exact precursors of erythrocytes and megakaryocytes will accelerate this effort.
- Being able to isolate lineage-specific blood cell progenitors will facilitate repairing genetic defects in patients using CRISPR-based methods (Doudna and Charpentier, 2014). It is likely to be important to target specific cell populations when DNA is edited.

Acknowledgement

The author is supported by the intramural research program of NIDCR, NIH.

References

Ackermann M, Liebhaber S, Klusmann JH, Lachmann N (2015). Lost in translation: pluripotent stem cell-derived hematopoiesis. *EMBO Mol Med* **7**: 1388–1402.

Adolfsson J, Mansson R, Buza-Vidas N *et al* (2005). Identification of Flt3+ lympho-myeloid stem cells lacking erythro-megakaryocytic potential a revised road map for adult blood lineage commitment. *Cell* **121**: 295–306.

Akashi K, Traver D, Miyamoto T, Weissman IL (2000). A clonogenic common myeloid progenitor that gives rise to all myeloid lineages. *Nature* **404**: 193–197.

Al-Drees MA, Yeo JH, Boumelhem BB *et al* (2015). Making blood: the haematopoietic niche throughout ontogeny. *Stem Cells Int* **2015**: 571893.

Barminko J, Reinholt B, Baron MH (2015). Development and differentiation of the erythroid lineage in mammals. *Dev Comp Immunol* doi: 10.1016/j.dci.2015.12.012.

Bensinger WI, Clift RA, Anasetti C *et al* (1996). Transplantation of allogeneic peripheral blood stem cells mobilized by recombinant human granulocyte colony stimulating factor. *Stem Cells* **14**: 90–105.

Doudna JA, Charpentier E (2014). Genome editing. The new frontier of genome engineering with CRISPR-Cas9. *Science* **346**: 1258096.

Kondo M, Weissman IL, Akashi K (1997). Identification of clonogenic common lymphoid progenitors in mouse bone marrow. *Cell* **91**: 661–672.

Mansson R, Hultquist A, Luc S *et al* (2007). Molecular evidence for hierarchical transcriptional lineage priming in fetal and adult stem cells and multipotent progenitors. *Immunity* **26**: 407–419.

Manz MG, Miyamoto T, Akashi K, Weissman IL (2002). Prospective isolation of human clonogenic common myeloid progenitors. *Proc Natl Acad Sci USA* **99**: 11872–11877.

Notta F, Zandi S, Takayama N *et al* (2015). Distinct routes of lineage development reshape the human blood hierarchy across ontogeny. *Science* doi: 10.1126/science.aab2116.

Ogawa M (1993). Differentiation and proliferation of hematopoietic stem cells. *Blood* **81**: 2844–2853.

Ramalho-Santos M, Willenbring H (2007). On the origin of the term "stem cell". *Cell Stem Cell* **1**: 35–38.

Shpall EJ, Wheeler CA, Turner SA *et al* (1999). A randomized phase 3 study of peripheral blood progenitor cell mobilization with stem cell factor and filgrastim in high-risk breast cancer patients. *Blood* **93**: 2491–2501.

Till JE, McCulloch EA, Siminovitch L (1964). A stochastic model of stem cell proliferation, based on the growth of spleen colony-forming cells. *Proc Natl Acad Sci USA* **51**: 29–36.

Yamanaka S (2007). Strategies and new developments in the generation of patient-specific pluripotent stem cells. *Cell Stem Cell* **1**: 39–49.

RESEARCH ARTICLE SUMMARY

HEMATOPOIESIS

Distinct routes of lineage development reshape the human blood hierarchy across ontogeny

Faiyaz Notta,* Sasan Zandi,* Naoya Takayama, Stephanie Dobson, Olga I. Gan, Gavin Wilson, Kerstin B. Kaufmann, Jessica McLeod, Elisa Laurenti, Cyrille F. Dunant, John D. McPherson, Lincoln D. Stein, Yigal Dror, John E. Dick†

INTRODUCTION: The hematopoietic road map is a compilation of the various lineage differentiation routes that a stem cell takes to make blood. This program produces greater than 10 blood cell fates and is responsible for generating more than 300 billion cells daily. On several occasions over the past six decades, the murine road map has been reconceived due to new information overturning dogma. However, the human road map has changed little. In the human model, blood differentiation initiates at the level of multipotent stem cells and passes through a series of increasingly lineage-restricted oligopotent and, finally, unipotent progenitor intermediates. One critical oligopotent intermediate is the common myeloid progenitor (CMP), believed to be the origin of all myeloid (My), erythroid (Er), and megakaryocyte (Mk) cells. Although murine studies challenge the existence of oligopotent progenitors, a comprehensive analysis of human My-Er-Mk differentiation is lacking. Moreover, whether the pool of oligopotent intermediates is fixed across human development (fetal to adult) is unknown.

RATIONALE: The differentiation road map taken by human hematopoietic stem cells (HSCs) is fundamental to our understanding of blood homeostasis, hematopoietic malignancies, and regenerative medicine.

RESULTS: We mapped the cellular origins of My, Er, and Mk lineages across three time points in human blood development: fetal liver (FL), neonatal cord blood (CB), and adult bone marrow (BM). Using a cell-sorting scheme based on markers linked to Er and Mk lineage specification (CD71 and CD110), we found that previously described populations of multipotent progenitors (MPPs), CMPs, and megakaryocyte-erythroid progenitors (MEPs) were heterogeneous and could be further purified. Nearly 3000 single cells from 11 cellular subsets from the $CD34^+$ compartment of FL, CB, and BM (33 subsets in total) were evaluated for their My, Er, and Mk lineage potential using an optimized single-cell assay.

In FL, the ratio of cells with multilineage versus unilineage potential remained constant in both the stem cell ($CD34^+CD38^-$) and progenitor cell ($CD34^+CD38^+$) enriched compartments. By contrast, in BM, nearly all multipotent cells were restricted to the stem cell compartment, whereas unilineage progenitors dominated the progenitor cell compartment. Oligopotent progenitors were only a negligible component of the human blood hierarchy in BM, leading to the inference that multipotent cells differentiate into unipotent cells directly by adulthood.

Mk/Er activity predominantly originated from the stem cell compartment at all developmental time points. In CB and BM, most Mks emerged as part of mixed clones from HSCs/MPPs, indicating that Mks directly branch from a multipotent cell and not from oligopotent progenitors like CMP. In FL, an almost pure Mk/Er progenitor was identified in the stem cell compartment, although less potent Mk/Er progenitors were also present in the progenitor compartment. In a hematological condition of HSC loss (aplastic anemia), Mk/Er but not My progenitors were more severely depleted, pinpointing a close physiological connection between HSC and the Mk/Er lineage.

ON OUR WEB SITE

Read the full article at http://dx.doi.org/10.1126/science.aab2116

CONCLUSION: Our data indicate that there are distinct road maps of blood differentiation across human development. Prenatally, Mk/Er lineage branching occurs throughout the cellular hierarchy. By adulthood, both Mk/Er activity and multipotency are restricted to the stem cell compartment, whereas the progenitor compartment is composed of unilineage progenitors forming a "two-tier" system, with few intervening oligopotent intermediates. ■

The list of author affiliations is available in the full article online.
*These authors contributed equally to this work.
†Corresponding author. E-mail: jdick@uhnres.utoronto.ca
Cite this article as F. Notta *et al.*, *Science* 351, aab2116 (2016). DOI: 10.1126/science.aab2116

Road maps of human blood stem cell differentiation. The classical model envisions that oligopotent progenitors such as CMP are an essential intermediate stage from which My/Er/Mk differentiation originates. The redefined model proposes a developmental shift in the progenitor cell architecture from the fetus, where many stem and progenitor cell types are multipotent, to the adult, where the stem cell compartment is multipotent but the progenitors are unipotent. The grayed planes represent theoretical tiers of differentiation.

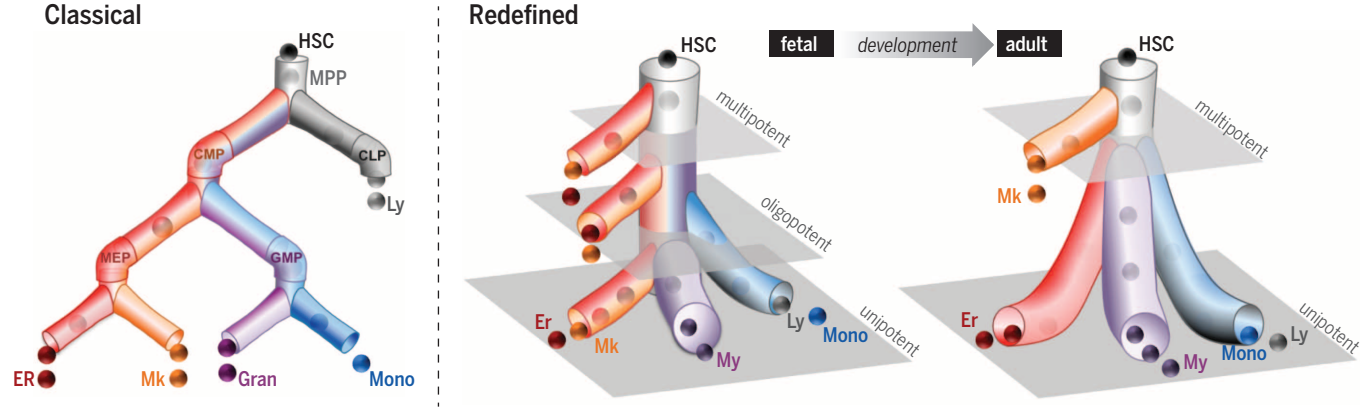

RESEARCH ARTICLE

HEMATOPOIESIS

Distinct routes of lineage development reshape the human blood hierarchy across ontogeny

Faiyaz Notta,[1,2]*† Sasan Zandi,[1,2]* Naoya Takayama,[1,2] Stephanie Dobson,[1,2] Olga I. Gan,[1] Gavin Wilson,[2,4] Kerstin B. Kaufmann,[1,2] Jessica McLeod,[1] Elisa Laurenti,[6] Cyrille F. Dunant,[7] John D. McPherson,[3,4] Lincoln D. Stein,[2,4] Yigal Dror,[5] John E. Dick[1,2]‡

In a classical view of hematopoiesis, the various blood cell lineages arise via a hierarchical scheme starting with multipotent stem cells that become increasingly restricted in their differentiation potential through oligopotent and then unipotent progenitors. We developed a cell-sorting scheme to resolve myeloid (My), erythroid (Er), and megakaryocytic (Mk) fates from single CD34$^+$ cells and then mapped the progenitor hierarchy across human development. Fetal liver contained large numbers of distinct oligopotent progenitors with intermingled My, Er, and Mk fates. However, few oligopotent progenitor intermediates were present in the adult bone marrow. Instead, only two progenitor classes predominate, multipotent and unipotent, with Er-Mk lineages emerging from multipotent cells. The developmental shift to an adult "two-tier" hierarchy challenges current dogma and provides a revised framework to understand normal and disease states of human hematopoiesis.

For decades, both human and mouse hematopoiesis has been described as a cellular hierarchy maintained by self-renewing hematopoietic stem cells (HSCs) that reside at the apex of its pyramidal structure of differentiating cells (*1*, *2*). This differentiation scheme highlights key features of the blood hierarchy that has been critical to our understanding of how stem cells manage lifelong blood production. In general, self-renewing cell types with extended life span like long-term HSCs (LT-HSCs), as well as short-term HSCs (ST-HSCs) and multipotent progenitors (MPPs), are rare and remain closer to the conceptual peak of the hierarchy; oligopotent and unipotent progenitors farther down the scheme have shorter life spans, increase numerically, and ultimately differentiate into more than 10 functional blood cell types. In the standard model of hematopoiesis, hierarchical differentiation commences from HSCs with the production of stem cell intermediates with less durable self-renewal potential that culminate with the generation of MPPs, the penultimate step before lineage specification. From MPPs, the common lineages for myelopoiesis [common myeloid progenitor (CMP)] and lymphopoiesis [common lymphoid progenitor (CLP)] are segregated (*3*, *4*). In myeloid (My) (defined herein as granulocyte/monocyte) differentiation, oligopotent CMPs undergo further restriction into bivalent granulocyte-monocyte progenitor (GMPs) that go on to make granulocytes and monocytes, and megakaryocyte-erythroid progenitors (MEPs) that go on to make platelets and red blood cells (RBCs). Thus, CMPs represent the critical oligopotent progenitor from which all My, erythroid (Er), and megakaryocyte (Mk) cells arise. Although the standard model is still used extensively as an operational paradigm, further cell purification and functional clonal assays have led to key revisions to the model. In mouse, the identification of lymphoid-primed multipotent progenitors (LMPPs) argued that Mk-Er potential must be the first lineage branch lost in lymphomyeloid specification of HSCs (*5*, *6*). Recently, paired-daughter analysis monitoring of mouse HSC cell divisions have demonstrated that Mk-Er progenitors can be derived from HSC directly without progressing through conventional MPPs and CMPs (*7*). Although these data challenge the standard model, clear consensus on a revised model of hematopoiesis is still lacking. Human hematopoiesis is widely regarded as following the same differentiation scheme as mouse hematopoiesis [reviewed in (*8*)]. Early work involving cell purification and methylcellulose (MC) colony-forming cell (CFC) assays identified CMPs and CLPs (*9*, *10*). However, purification schemes to resolve My, Er, Mk, and lymphoid (Ly) fates remained poor. Through the development of more efficient assays to monitor Ly fates in single-cell stromal assays and an improved sorting scheme, we identified human multilymphoid progenitors (MLPs) as the earliest lymphoid differentiation precursor with concomitant lymphoid (T, B, and natural killer) and myelomonocytic potential (*11*, *12*). Considerable uncertainty remains concerning the myelo-erythro-megakaryocytic branch of human hematopoiesis because clonogenic CFC assays do not read out My, Er, and Mk fates efficiently or contemporaneously, making it difficult to account for all cells within phenotypically pure populations of CMPs and MEPs. A comprehensive analysis of human myelo-erythro-megakaryocytic development has not been undertaken, so it is really only by default that the standard model applies.

Much of our understanding of the molecular basis of cellular differentiation and lineage commitment is derived from the assumptions implicit in the standard model. For example, simultaneous expression of molecular factors associated with My-Er-Mk lineages at low levels is considered to maintain CMPs as the origin of the common lineage for myelopoiesis (*3*). During lineage restriction to GMPs and MEPs, progressive upregulation of particular lineage factors initiates feedforward and feedback molecular controls that lock in a granulocyte/monocyte or a Mk-Er differentiation program. An important axiom that arises from this molecular view of the standard model is that cellular differentiation is gradual. However, transcriptional studies of highly purified or single-cell murine HSC has established that molecular programs corresponding to My-Er-Mk fates can directly emerge in multipotent cells, arguing that cellular differentiation is not gradual and that myeloid differentiation can occur without progressing through an intermediate CMP stage (*6*, *7*, *13*–*17*). Naik *et al.* have demonstrated that nearly half of the LMPP compartment is biased toward dendritic cell commitment, a lineage previously thought to come from the CMP-to-GMP route (*15*). Molecular factors associated with Mk-Er differentiation have been shown to be active in LT-HSCs (*13*, *14*), and prospective isolation of platelet-biased LT-HSCs strongly supports that this lineage is not derived from the CMP to MEP route (*16*). Whether molecular programs that regulate My-Er-Mk fates arise at the level of HSCs in humans is not known. It is important to understand where Er and Mk lineage branching occurs in the human hematopoietic hierarchy because these lineages comprise 99% of the cellular component of blood and represent the bulk of the 300 billion blood cells that turn over daily in humans. Mapping the cellular origins of Er and Mk lineages in the human blood hierarchy represents a critical step to define the molecular basis of their fate commitment.

The cellular road map describing the blood hierarchy has been built on two core experimental pillars: cell purification and clonal assays. Human

[1]Princess Margaret Cancer Centre, University Health Network, University of Toronto, Toronto, Ontario, Canada. [2]Department of Molecular Genetics, University of Toronto, Toronto, Ontario, Canada. [3]Medical Biophysics, University of Toronto, Toronto, Ontario, Canada. [4]Ontario Institute for Cancer Research, Toronto, Ontario, Canada. [5]The Hospital for Sick Children Research Institute, University of Toronto, Ontario, Canada. [6]Wellcome Trust, Medical Research Council Cambridge Stem Cell Institute, Department of Haematology, University of Cambridge, Cambridge, UK. [7]Ecole Polytechnique Fédérale de Lausanne, LMC, Station 12, Lausanne, CH-1015, Switzerland.
*These authors contributed equally to this work. †Present address: Ontario Institute for Cancer Research, Toronto, Ontario, Canada.
‡Corresponding author. E-mail: jdick@uhnres.utoronto.ca

studies reporting on sorting schemes for the myelo-erythroid progenitor hierarchy (CMPs, GMPs, and MEPs) have often assumed that "marker-pure" subsets are synonymous with "functionally pure" subsets (*9*). In other words, each cell within the purified subset possesses the same differentiation potential (Fig. 1A, 1). This interpretation is primarily derived from clonogenic assessment of human CMPs, GMPs, and MEPs using standard CFC assays. In CFC assays, purified CMPs typically generate My, Er, or Mk colonies; GMPs give rise to My colonies only; and MEPs give rise to Er and/or Mks (*9*). Because CMPs displayed all lineage readouts, whereas GMPs and MEPs did not, CMPs were interpreted as both marker-pure and functionally pure on the basis that the CFC assay was inefficient in being able to read out mixed differentiation potential. This reasoning underpins the basic bifurcating scheme of human CMPs to GMPs and MEPs. However, an alternate interpretation exists if we assume that the CFC assay is actually efficient. In this case, human CMPs are phenotypically homogenous (e.g., marker-pure) but are functionally heterogeneous, consisting of diverse unipotent progenitors (Fig. 1A, 2). This contention could only be proven if a new sorting strategy is able to isolate, in functionally pure form, each type of the unilineage progenitor from the starting CMP population. To distinguish between the two alternatives, we need (i) a new sorting strategy for human myelo-erythroid progenitors, and (ii) a more sensitive assay to assess mixed cell potential. Until both scenarios can be experimentally resolved, there is considerable uncertainty that clouds the classical view of the human hematopoietic hierarchy. We attempted to address both of these issues by developing a cell-sorting scheme and an optimized single-cell assay to efficiently read out My, Er, and Mk fates from putative multilineage cell types.

Results

Previously defined human MPPs, CMPs, and MEPs are heterogeneous

We developed a cell-sorting scheme to examine the cellular heterogeneity within the $CD34^+$ compartment of human blood. To a previous seven-parameter design (CD34, CD38, CD7, CD10, FLT3, CD45RA, and Thy1) (*11*), we distinguished HSCs from MPPs by adding CD49f (*18*); identified Er-Mk progenitors by adding cMPL (CD110) (*19*, *20*) (designated here as BAH1 to be consistent with the antibody clone used to detect this antigen) (*21*, *22*) and CD71 (transferrin receptor); and distinguished B-lymphoid–committed progenitors from My progenitors, such as GMPs in the $CD45RA^+$ fraction, by adding CD19. Upon evaluation in human fetal liver (FL), neonatal cord blood (CB), and adult bone marrow (BM), this 11-parameter cell-sorting layout provided a high-resolution view of the phenotypic heterogeneity that exists within $CD34^+$ cells across all developmental stages (Fig. 1B and fig. S1).

Many distinct cell types, such as HSCs, MPPs, and MLPs, reside within the $CD34^+CD38^-/lo$ (simplified as $CD34^+CD38^-$ herein) stem cell–enriched compartment of human blood. We investigated whether CD71 or BAH1 expression corresponded to a known cell type within this compartment in the FL. About 10% of the FL $CD34^+CD38^-$ expressed CD71, and half of these $CD71^+$ cells also expressed BAH1 (fig. S1A, 2). Neither CD71 nor BAH1 was expressed on $Thy1^+$ HSCs (fig. S2A) or on $CD45RA^+$ MLPs (fig. S2B), which suggests that these markers identify a different cell type within the MPP compartment. We redefined the current MPP compartment into three fractions (F1, F2, and F3) on the basis of CD71 and BAH1 expression: MPP F1 cells were $CD71^-BAH1^-$, MPP F2 cells were $CD71^+BAH1^-$, and MPP F3 cells were $CD71^+BAH1^+$ (Fig. 1B, vii). The expression of these molecules in the $CD34^+CD38^-$ compartment was unexpected because the onset of Mk-Er lineage commitment according to the standard model occurs at the level of CMPs and MEPs that are found in the progenitor-enriched $CD34^+CD38^+$ compartment. These data suggest that the detection of functional Er and Mk differentiation molecules on a subset of $CD34^+CD38^-$ cells represents a unique Mk-Er branch point within the multilineage compartment.

We next analyzed CD71 and BAH1 expression in the $CD34^+CD38^+$ progenitor compartment. Co-expression of FLT3 and the lymphoid antigen CD7 in FL $CD34^+CD38^+$ cells (fig. S2C) indicated that CD7 expression is not exclusive to lymphoid progenitors as reported previously in CB (*23*). Thus, CD7-expressing cells were not excluded in our sorting layout. In lieu of CD7, we used CD10 expression to exclude Ly progenitors (Fig. 1B, i; fig. S1, 6). In the FL $CD34^+CD38^+CD10^-$ cell compartment, FLT3 and CD45RA expression

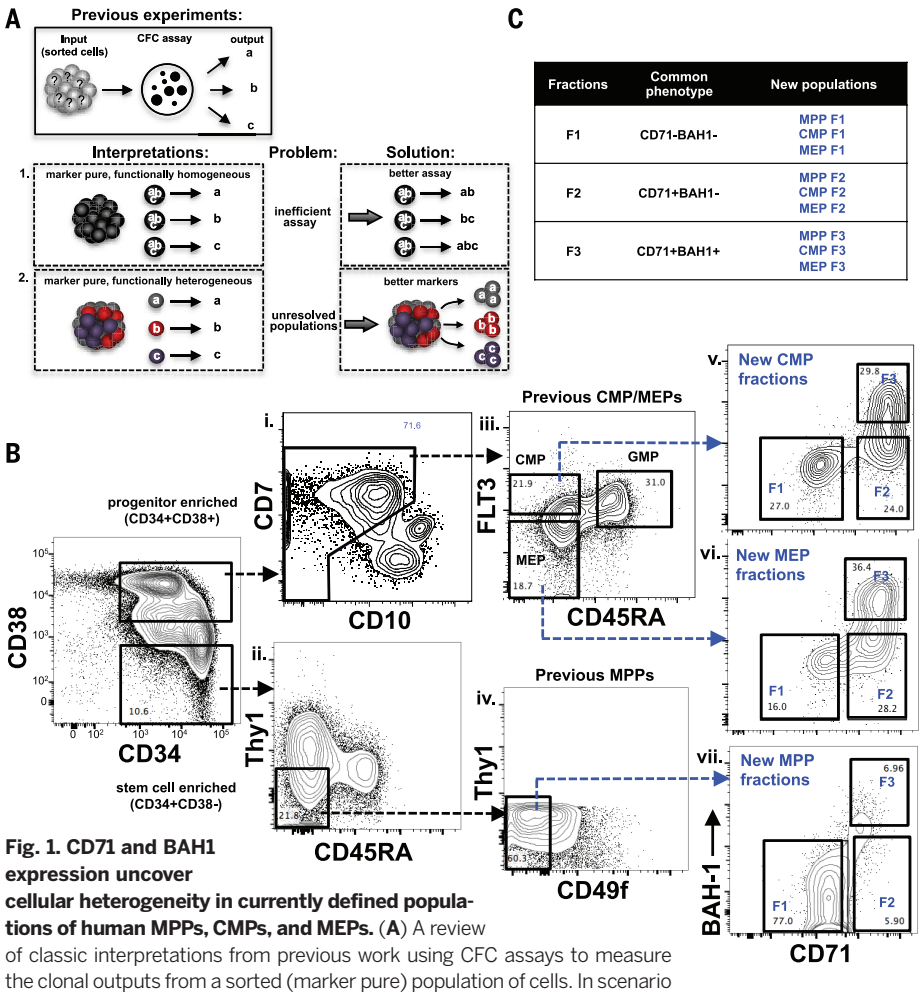

Fig. 1. CD71 and BAH1 expression uncover cellular heterogeneity in currently defined populations of human MPPs, CMPs, and MEPs. (**A**) A review of classic interpretations from previous work using CFC assays to measure the clonal outputs from a sorted (marker pure) population of cells. In scenario 1, each cell within a marker-pure population has the potential to give rise to three functional outputs (a, b, and c) but only gives rise to one of them in the assay. Under this condition, diverse functional outputs from a marker-pure population are interpreted to be derived from a functionally homogeneous population of multilineage cells. In the alternate scenario 2, a marker-pure population is composed of three distinct unipotent cell types that give rise to lineages a, b, and c independently. Both of these scenarios can be reconciled with a better assay (right top) or better markers (right bottom). (**B**) The gating scheme of defining MPPs ($CD34^+CD38^-Thy1^-CD45RA^-CD49f^-$), CMPs ($CD34^+CD38^+CD10^-FLT3^+CD45RA^-$), and MEPs ($CD34^+CD38^+CD10^-FLT3CD45RA^-$) from a representative human FL sample is shown (black dashed arrows). MPPs, CMPs, and MEPs were further divided into F1 ($CD71^-BAH1^-$), F2 ($CD71^+BAH1^-$), and F3 ($CD71^+BAH1^+$) (blue dashed arrows). Full gating scheme for FL, CB, and BM $CD34^+$ cells is presented in fig. S1. (**C**) Summary of the new subsets used in this study.

was used to identify commonly defined CMPs ($FLT3^+CD45RA^-$), GMPs ($FLT3^+CD45RA^+$), and MEPs ($FLT3^-CD45RA^-$) (Fig. 1B, iii; fig. S1, 7). Addition of CD71 and BAH1 to CMP and MEP populations uncovered phenotypic heterogeneity within these populations previously considered to be homogeneous. In line with the nomenclature we used for the redefined MPP compartment described above, CMP and MEP compartments were also subdivided into three fractions with CD71 and BAH1 (F1, $CD71^-BAH1^-$; F2, $CD71^+BAH1^-$; F3, $CD71^+BAH1^+$) (Fig. 1B, v to vii, and fig. S1, panels 8 and 10). We repeated the same analysis in CB and adult BM to determine whether CB and adult BM samples were similarly heterogeneous. All the major cell populations identified in the FL were also observed in CB and BM, albeit to different degrees (table S1), indicating that the cellular heterogeneity uncovered by CD71 and BAH1 existed across all developmental stages (fig. S1, B and C). Thus, previously defined human CMPs and MEPs that were considered homogeneous are in fact phenotypically heterogeneous when Er and Mk markers are applied.

In summary, previously defined MPPs, CMPs, and MEPs contain three distinct cellular fractions: F1, lacking CD71 and BAH1; F2, expressing CD71 but lacking BAH1; and F3, expressing both molecules. A total of 33 distinct cellular classes from FL, CB, and BM (11 per developmental stage) were functionally interrogated to evaluate their lineage fate potential. To facilitate the review of the results below, a legend and complete phenotype is provided in Fig. 1C and table S1.

An optimized single-cell assay for human My-Er-Mk progenitors

To evaluate the functional potential of the cellular subsets identified above, we developed a single-cell in vitro assay that overcame the shortcomings of previous approaches to characterize human myeloid progenitors. An ideal assay would support the ability of single cells to simultaneously commit along My, Er, and/or Mk fates, as well as to provide the conditions for their differentiated progeny to survive, propagate, and expand to permit detection. Standard MC assays do not strictly fulfill these criteria. For example, $CD49f^+$ HSCs exclusively generated CFU-My in MC (fig. S3A and supplementary text), yet single HSCs sustain multilineage hematopoiesis in vivo (*18*). Also, the limited self-renewal potential of downstream progenitors makes them difficult to read out in vivo at clonal resolution, further highlighting the need to develop more sensitive in vitro methodology to assess the lineage potential of progenitors. We found that serum-free conditions supplemented with growth factors (SCF, FLT3, TPO, EPO, IL-6, IL-3, IL-11, GM-CSF, and LDL) and stroma were highly efficient at assaying My, Er, and Mk lineage potential from single $CD34^+$ cells. Single-cell–derived clones were analyzed by flow cytometry after a 2- to 3-week culture period for Mk (CD41 and CD42b), Er (GlyA), and My (CD14, CD15, and CD33) cells. One example of the efficiency of this new assay comes from the analysis of the $CD49f^+$ HSC subset, which previously could not be read out in vitro as single cells (*11*). Under these new conditions, 77% of FL, 72% of CB, and 48% of BM single $CD49f^+$ HSCs were able to produce a clone (fig. S5A, left). Whereas only CFU-My were produced from HSC in MC, mixed clonogenic potential was now readily detectable with this assay. We used this assay to functionally map the lineage potential of all the newly defined $CD34^+$ subsets from all three developmental time points.

Unipotent progenitors dominate the blood hierarchy by adulthood

To gain a global perspective of the functional differences in the blood hierarchy across ontogeny, we first combined all 11 $CD34^+$ subsets from each developmental time point into one analysis of nearly 3000 single cells. Cloning efficiency was highest for FL and decreased gradually in CB and BM (FL, 74%; CB, 69%; BM, 55%) (Fig. 2A). A simple stratification based on whether a single cell gave rise to one (unilineage) or more (multilineage) cell lineages revealed that 40% of FL $CD34^+$ cells were multilineage compared with 27% of CB ($P < 10^{-3}$, Fisher's exact test) and 18% of BM ($P < 10^{-3}$, Fisher's exact test) $CD34^+$ cells (Fig. 2B). Thus, the ratio of multilineage to unilineage progenitors changes en bloc in development within the $CD34^+$ population, a result that is independent of the complex marker scheme that we used.

To continue exploring the organizational relationships of progenitors across developmental time points, we investigated the proportion of multilineage to unilineage cells in the stem-cell–enriched ($CD34^+CD38^-$) and the progenitor-enriched ($CD34^+CD38^+$) subsets. Within $CD34^+CD38^-$ cells, FL and CB had a significantly higher proportion of multilineage cells compared with BM (FL versus BM: 48.6% versus 32.9%, $P = 0.0016$; CB versus BM: 46.1% versus 32.9%, $P = 0.011$; Fisher's exact test). These proportional differences were more pronounced in the $CD34^+CD38^+$ progenitor compartment. In $CD34^+CD38^+$ cells, BM displayed a factor of 3 fewer multilineage cells compared with FL (FL, 28.8%; CB, 17.3%; BM, 9.6%; $P < 0.0001$, Fisher's exact test) (Fig. 2, C and D). Thus, both the stem and progenitor compartments from each developmental stage exhibited a proportional

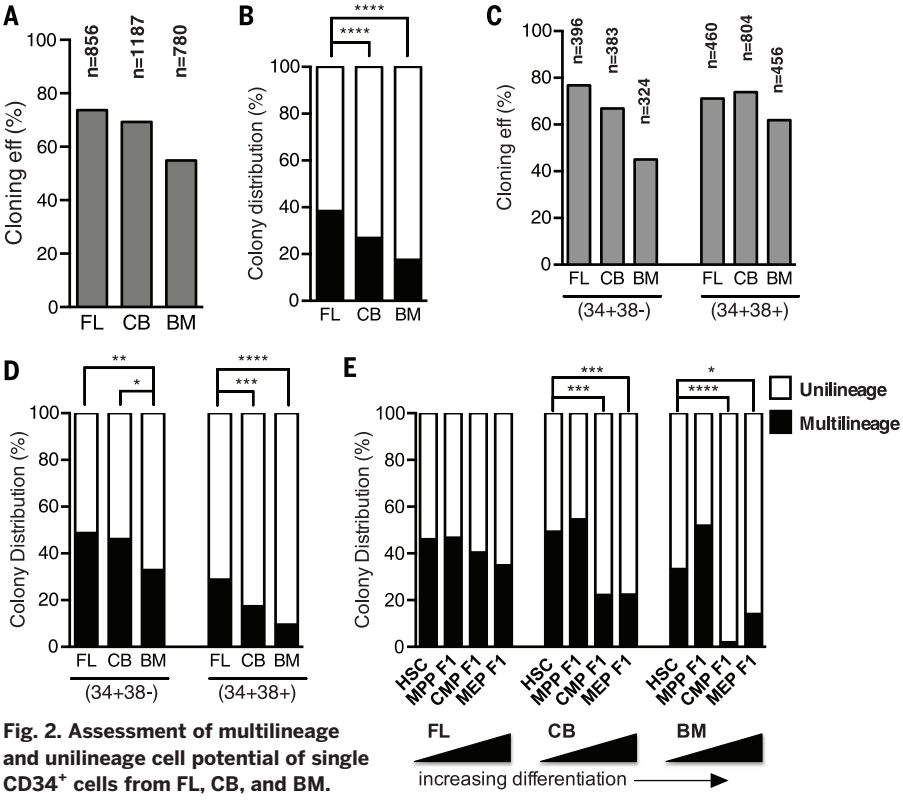

Fig. 2. Assessment of multilineage and unilineage cell potential of single $CD34^+$ cells from FL, CB, and BM.
(**A** to **D**) Single cells from subsets defined in Fig. 1C were deposited by fluorescence-activated cell sorting (FACS) and cultured for several weeks. Emergent clones were analyzed by flow cytometry for My, Er, and Mk lineages (Fig. 3A). To gain a global perspective of the functional differences between FL, CB, and BM, subsets were combined into one analysis of $CD34^+$ cells [(A) and (B)] or stem ($CD34^+CD38^-$) and progenitor ($CD34^+CD38^+$) cell compartments [(C) and (D)]. A single cell was defined as multilineage (black) when it gave rise to more than one lineage (any two of My, Er, or Mk) and unipotent when it gave rise to one lineage (My or Er or Mk) [(B) and (D)]. Overall cloning efficiency is shown in gray [(A) and (C)]. (**E**) Distribution of multilineage and unilineage cell potential from populations that lack CD71 and BAH-1 (F1) expression (shown by increasing differentiation: HSC > MPP F1 > CMP F1 > MEP F1). Asterisks indicate significance based on Fisher's exact test (*$P < 0.05$, **$P < 0.01$, ***$P < 0.001$, ****$P < 0.0001$).

change in the percentage of multilineage cell types.

Next, we localized the differentiation stages most affected by the loss of multilineage progenitors. We reasoned that HSCs and subsets that lack differentiation markers CD71 and BAH1 (MPP F1, CMP F1, and MEP F1) would be enriched for cells with multilineage cell potential. Notably, in FL, the ratio of multilineage to unilineage progenitors remained nearly constant across these subsets (Fig. 2E). By contrast, only HSC and MPP F1 subsets from CB and BM were highly enriched for multilineage cells, whereas their corresponding CMP/MEP F1s were composed mostly of unilineage cell types (Fig. 2E; $P < 0.05$, Fisher's exact test). In BM, virtually all multilineage cells were restricted to the $CD34^+CD38^-$ stem cell compartment (Fig. 2E; $P < 0.05$, Fisher's exact test). Hence, multilineage cell potential extends into the progenitor compartment in FL, but in BM, this potential is restricted to the $CD34^+CD38^-$ stem cell compartment. In parallel, the progenitor compartment in BM is dominated by unilineage cell types.

Mk-Er lineage branching in the blood hierarchy is developmentally defined

To gain a detailed understanding of the differentiation potential of each progenitor subset identified by our sorting scheme applied to FL, CB, and BM, we classified the functional potential of each single cell in our data set. Five distinct clonal outputs were classified: Mk only, Er only, My only, Mk/Er, and mixed (bipotent, Er/My or Mk/My; tripotent, Er/Mk/My) (Fig. 3A). The cloning efficiency of all subsets was high in MPP, CMP, and MEP fractions (50 to 80%) (Fig. 3B and fig. S5A).

The highest percentage of mixed clones was found among the HSC subsets (FL, 46.1%; CB, 49.3; BM, 33.3%) (fig. S5A), except in BM, where MPP F1 harbored higher mixed clone potential than HSC (51.9%), although this was not significant (BM HSC versus MPP F1: $P = 0.1$, Fisher's exact test) (Fig. 2E). FL HSC and MPP F1 subsets had a statistically higher distribution of tripotent versus bipotent mixed clones compared with CB and BM HSC and MPP F1 (fig. S5B). In FL and CB, Mk-Er-only clones appeared at the MPP F1 stage (FL, 29% of total; CB, 18% of total) (Fig. 3B, column 1, row 1). In BM, Mk-Er clones from MPP F1 were rare (~2%); rather, 15% of all clones from this subset were Er-only. Mk activity from BM MPP F1 was detected as a component of mixed clones that also contained My cells (further discussed below).

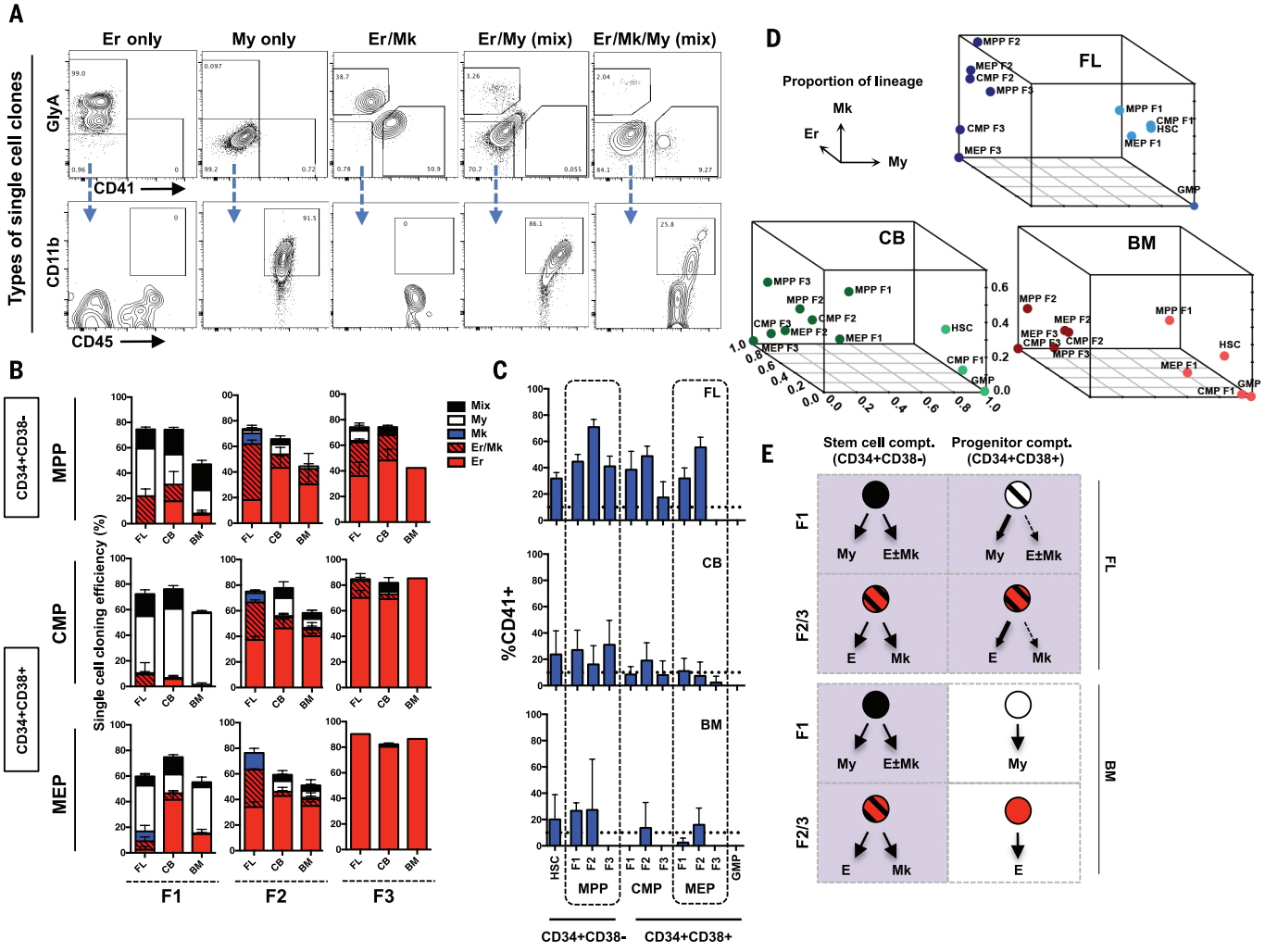

Fig. 3. Lineage analysis of single-cell clones from subfractions of MPP, CMP, and MEP populations. (**A**) Single-cell clones were analyzed by flow cytometry and binned into five distinct lineage outcomes. Erythroid clones were defined as $GlyA^+$ only (Er only). Myeloid clones were identified as $GlyA^-CD41^-$ but $CD45^+CD11b^+$ (My only). Erythroid-megakaryocyte clones were defined as $GlyA^+$ and $CD41^+$ but negative for CD11b (Er/Mk). Mix clones were defined My and Er or Mk (column 4) or My, Er, and Mk (column 5). (**B**) Cloning efficiency and lineage outcomes of single cells from newly defined MPP, CMP, and MEP fractions (F1, F2, and F3) from FL, CB, and BM. (**C**) Total Mk output ($CD41^+$) from all newly defined subsets from FL, CB, and BM. Bars indicate mean ± SE. Total number of independent experiments: $n = 3$, 6, and 4 for FL, CB, and BM, respectively. The dotted line defines the threshold for detecting positive Mk lineage potential from a sorted fraction due to analytical noise that arises from single clone flow cytometry. (**D**) Three-dimensional summary of lineage outputs (My, Er, and Mk) from all cellular subsets in FL, CB, and BM presented in (B). (**E**) Pictorial depiction of the predominant lineage outcomes from stem ($CD34^+CD38^-$) and progenitor ($CD34^+CD38^+$) cell compartments in FL and BM data.

We next interrogated the $CD34^+CD38^+$ compartment. Based on the classical view of the blood hierarchy, we would expect that true CMPs reside in a subset that lacks expression of differentiation markers such as CD71 and BAH1 (CMP F1). Only 15% of FL and CB CMP F1 clones were mixed, and no mixed clones from this subset were detected in BM (Fig. 3B, column 1, row 2). Thus, we conclude that previously defined BM CMPs are not homogeneous for cells with multilineage My-Er-Mk potential; rather, they are heterogeneous and composed of subpopulations of unilineage My, Er, and Mk progenitors (Fig. 3B, row 2). To determine whether the small percentage of mixed clones from FL and CB CMPs F1 population were derived from bona fide CMPs, we evaluated their My-Er-Mk potential. More than 80% of the mixed clones from FL and CB were bipotent (either Er/My or Mk/My) without concurrent Mk-Er-My potential (fig. S5C). These data demonstrate that bona fide CMPs are a rare component of the human hematopoietic tree, irrespective of developmental stage.

MC and megacult colony assays indicated that subsets defined by CD71 and BAH1 expression (F2 and F3) were highly enriched for Mk and Er activity (fig. S3, A to D, and supplementary text). However, these assays cannot formally rule out that Er and Mk potential was derived from independent unilineage progenitors. We first tracked Mk-Er activity from single cells within the MEP subsets (MEP F1 through F3) (Fig. 3B, row 3). MEP F1 was highly heterogeneous across developmental time points and composed mostly of My progenitors in FL and BM (60% or more) (Fig. 3B, column 1, row 3) that functionally resemble other F1 subsets from MPPs and CMPs. In CB and BM, ~70% of clones from MEP F2 were Er-only, and 10% or less were Mk-Er clones (Fig. 3B, column 2, row 3). MEP F2 is likely the subset within classical MEPs that gave rise to low-level Mk colonies in previous studies. MEP F3, the numerically dominant cell population within the classical MEPs, uniformly produced Er-only clones in FL, CB, and BM (Fig. 3B, column 3, row 3). Thus, classically defined MEPs are principally composed of Er-only progenitors when analyzed at single-cell resolution and are not Mk-Er progenitors as previously thought.

As only rare cells within the MEP fractions give rise to Mks, Mk potential must lie elsewhere in the blood hierarchy. We found that most Mk-Er activity came from the $CD34^+CD38^-$ stem cell compartment (fig. S3C) and was particularly enriched within one of our newly defined MPP subsets (Fig. 3B, column 2, row 1). In FL, 60% of clones from MPP F2 were of Mk-Er type, and the remainder of this subset was composed of Mk-only or Er-only clones (Fig. 3B, column 2, row 1). Notably, Mk activity was enriched but not restricted to the stem cell compartment in the FL. Because we did not find strong evidence for FL CMPs, we expect that FL Mk-Er progenitors arise from the stem cell compartment, specifically from MPP F2. In CB and BM, Mk-Er clones represented one-quarter of the total clonal output from this subset (Fig. 3B, column 2, row 1), and the rest were Er-only clones. In CB—and more evident in BM—Mks predominantly emerged as part of mixed clones from HSCs and MPP F1, supporting the hypothesis that Mk branching occurs directly from a multipotent cell, as predicted by the murine studies (*7*). These data suggest that both Mk-Er and multilineage potential are restricted to the stem cell compartment by adulthood, whereas unilineage fates predominate the progenitor compartment, forming a simple "two-tier" hierarchy, with few intervening oligopotent intermediates (Fig. 3, D and E).

In vivo analysis establishes hierarchical relationships between progenitor subsets

In the blood hierarchy, cell types near the peak of the hierarchy, such as HSCs and MPPs, are rarer but possess higher proliferative potential. Lineage differentiation typically correlates with loss of proliferative potential. Although HSC and MPP subsets (F1 to F3) are minor populations, they yielded 5 to 10 times as many cells compared with more abundant populations from the CMP and MEP subsets in vitro (fig. S6A).

We then transplanted our cellular subsets in vivo and measured graft durability and size, as well as its lineage composition, to establish the hierarchical relationships of our newly defined progenitor subsets. Due to tissue availability, only CB was used. Because there are limited data on the engraftment capacity of human progenitors in the NOD-*Scid-Il2rg*^{null} (NSG) model, we first scrutinized the repopulation kinetics of human blood cells in this model. Using HSCs, we observed low-level lymphomyeloid as well as erythro-megakaryocytic engraftment as early as 2 weeks after transplant (fig. S6, B and C), consistent with previous studies using NOD-*Scid* mice (*24*). We used 2 weeks as the standpoint from which to assess progenitor cell engraftment in vivo. One thousand CMP F1 cells and 3000 MEP F1 cells generated a myelo-erythroid restricted graft that did not persist beyond 2 weeks (Fig. 4A, column 3 and 5, and fig. S6E). By contrast, 200 MPP F1 cells were able to sustain a robust and systemic multilineage graft (My-Er-Ly) beyond 2 weeks, consistent with the functional potential of true MPPs (Fig. 4A, column 1; Fig. 4B; and fig. S6E) (*18*).

To gather enough cell numbers for in vivo detection of Er-enriched subsets, we combined the F2 and F3 subsets from MPPs, CMPs, and MEPs for transplantation because they shared similar functional potential in vitro. The combined F2/F3 subsets from MPPs, CMPs, and MEPs all gave rise to prominent Er grafts in vivo, concordant with their in vitro potential (Fig. 4A, columns 2, 4, and 6; and fig. S6D, top panels). MPP F2/F3 cells were highly proliferative and generated a robust Er graft with only 400 transplanted cells

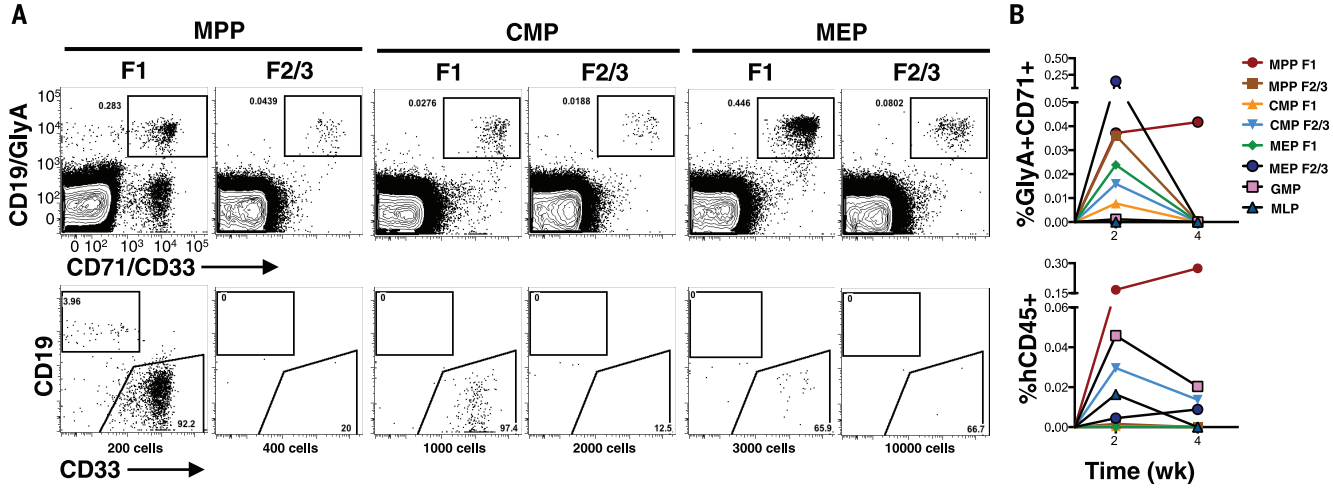

Fig. 4. In vivo potential of progenitor subsets. (**A**) Freshly sorted populations from CB were intrafemorally transplanted into sublethally irradiated NSG mice. Bone marrow from injected femur and noninjected bones were analyzed by flow cytometry 2 weeks after transplant. The average transplanted cell dose is shown at the bottom of the flow plot. Top row indicates Er engraftment ($GlyA^+CD71^+$). Bottom row indicates total human leukocyte engraftment ($CD45^+$). B-lymphoid cells and My cells were detected using CD19 and CD33, respectively. (**B**) Kinetic analysis of engraftment from progenitor subsets. Mean levels of Er ($GlyA^+CD71^+$) and total human cell engraftment ($CD45^+$) are shown.

(Fig. 4A, column 2), whereas CMP F2/F3 and MEP F2/F3 required cell doses higher by a factor of 5 to 25 to generate an in vivo graft (Fig. 4A, columns 4 and 6). Although platelets were difficult to detect in vivo from progenitor subsets, we did observe them in rare mice engrafted with either MPP F1 or MPP F2/3 cells (fig. S6C). Only MPP F2/F3, but not CMP F2/3 and MEP F2/3, were able to migrate systemically to nontransplanted bones and resemble the proliferative potential of MPP F1 (fig. S6E). When combined with the in vitro analyses of these subsets, these in vivo experiments support that Mk-Er-enriched MPP F2/F3 are derived from HSCs or MPPs directly without invoking a lineage route via a CMP intermediate.

A transcriptionally defined erythroid progenitor subnetwork in the CD34 hierarchy

Lineage commitment coincides with the expression of key molecules that aid to "lock in" a differentiation program (*25*). Using low-cell-input RNA-sequencing methodology (*26*), we first analyzed the expression profile of canonical lineage factors in bulk CB subsets. Genes associated with My specification, such as *MPO* and *CSF2RA* (*GM-CSFR*), were highly expressed in GMPs, whereas genes associated with the Er lineage, such as *GATA-1* and *EPOR*, were highly expressed in F2/F3 subsets from MPP, CMP, and MEP populations (fig. S7A). Mk differentiation markers, *CD41* (*ITGA2B*) and *CD42b* (*GP1BA*), were highly expressed in MPP F2, in line with the functional potential of this subset. These data provide an independent line of evidence that committed Mk progenitors reside within the stem cell compartment. Low-level expression of *CD41* and *CD42b* was also detected in MPP F3 and MEP F2, consistent with the residual Mk activity from these CB subsets (fig. S7A).

Unsupervised hierarchical clustering and principal component analysis of the entire data set revealed two major molecular subgroups: those with Er-enriched potential (MPP, CMP, and MEP F2/F3), and another with multilineage (HSC or MPP F1) or My-enriched potential (CMP F1 or MEP F1) (fig. S7B). F2 and F3 subsets within MPP, CMP, and MEP populations clustered together, suggesting that these pairs are more closely related within each broader compartment (fig. S7Bi). Due to their close transcriptional and functional relationship, we merged F2 and F3 subsets from MPP, CMP, and MEP subsets to compare global transcriptional differences among these Er-enriched subsets. We found that 230 genes were differentially expressed between MPP (F2/F3) versus CMP (F2/F3), and 52 genes between CMP (F2/F3) versus MEP (F2/F3). These differentially expressed genes were highly enriched in the cell cycle and DNA replication and metabolic processes, and coincide with the extensive proliferation that Er progenitors undergo during specification (fig. S7C). These data reinforce the idea that the close functional relationship between Mk-Er and Er enriched subsets is likely due to shared molecular programs.

Molecular heterogeneity among single cells within a purified subset is commonly lost in a population-level analysis. We tracked the expression of key lineage factors among single cells in our progenitor subsets. Only FL and BM were used in this experiment because they represent the two ends of the development time points used in this study. In both FL and BM, single cells from F2 and F3 from MPPs, CMPs, and MEPs displayed a dominant Er gene expression program, often co-expressing both *GATA1* and *EPOR* genes in the same cell (Fig. 5A and fig. S7D). Our sorting method

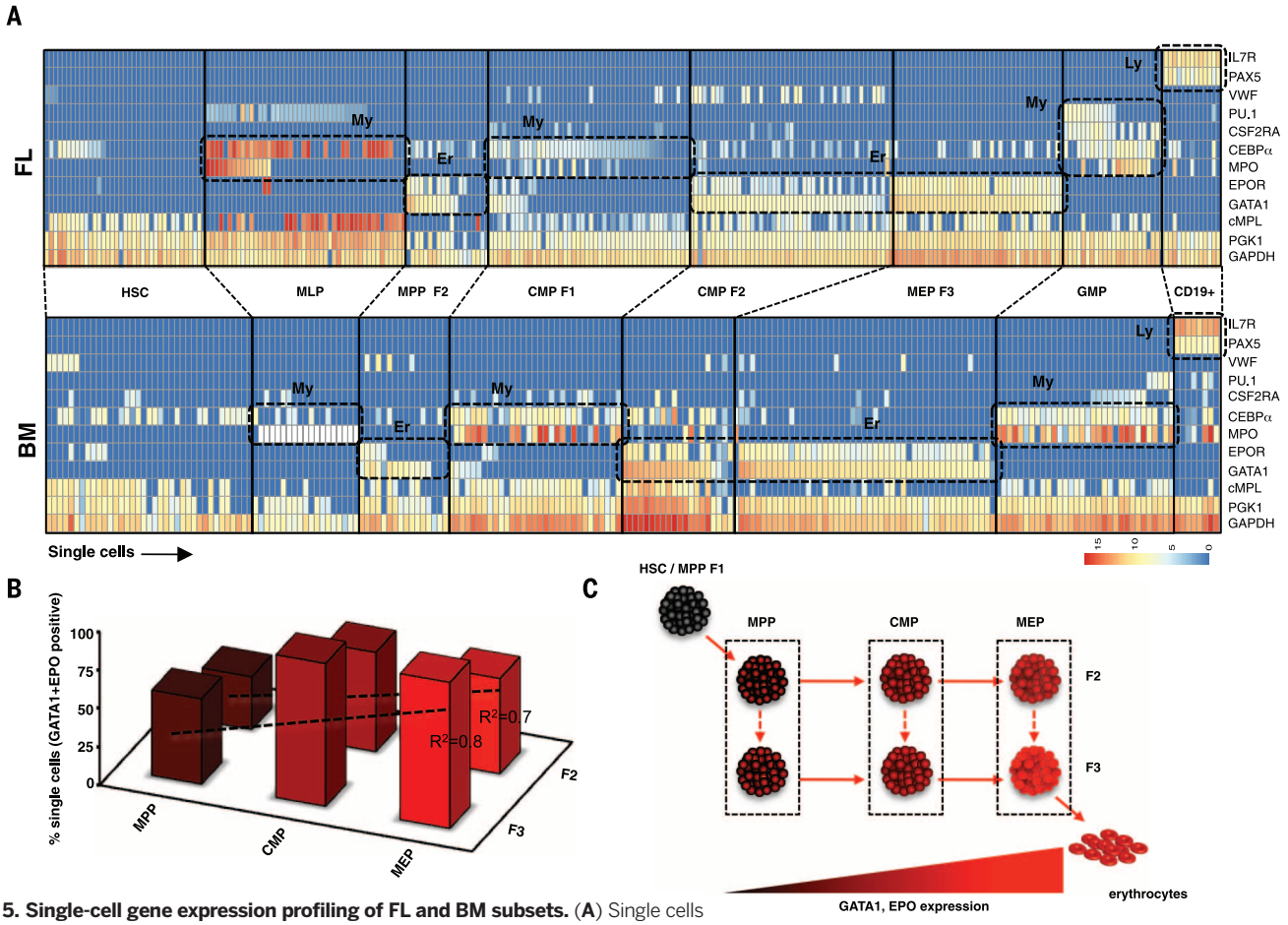

Fig. 5. Single-cell gene expression profiling of FL and BM subsets. (**A**) Single cells from FL (top) and BM (bottom) subsets were sorted and analyzed for expression of genes associated with My, Er, and Ly lineages (shown on right) on the Fluidigm platform. My, Er, or Ly gene clusters are shown as dashed boxes. (**B**) Percentage of single cells that coexpress *GATA1* and *EPOR* in F2 and F3 from MPP, CMP, and MEP subsets. BM and FL F2 and F3 subsets were combined in this analysis. (**C**) A theoretical subnetwork of Er progenitors within the $CD34^+$ compartment.

can essentially resolve the Er-committed progenitors within the CD34$^+$ hierarchy. We observed that *GATA1* expression was present among most single cells in MPP F2 and MPP F3, but *EPOR* expression was only present in a subset of *GATA1*-positive cells (Fig. 5, A and B). Because *GATA1* precedes *EPOR* expression in Er differentiation, MPP F2/F3 cells represent the earliest erythroid differentiation precursor in the human blood hierarchy. The percentage of single cells that co-expressed *GATA1* and *EPOR* increased in proportion among F2 and F3 subsets from MPPs, CMPs, and MEPs in both FL and BM (Fig. 5B). These molecular factors are considered a surrogate of the degree of Er differentiation (Fig. 5B). When considered jointly with our in vitro and in vivo analyses, these subsets are already Er-specified but vary mostly in their proliferative potential. We hypothesize that these subsets compose a hierarchical subnetwork of Er progenitors within the CD34$^+$ compartment (Fig. 5C). A candidate network map is shown in Fig. 5C. Because erythrocytes comprise nearly 99% of all blood cells, this network may offer a high degree of flexibility to synthesize erythrocytes under homeostatic and emergency erythropoiesis without HSC input.

Dramatic loss of Er progenitors compared with My progenitors in a hematologic condition of HSC deficiency

Recent HSC fate-mapping analyses in mice have provocatively shown that progenitors, but not HSCs, are fundamental for ongoing hematopoiesis under homeostatic conditions (*27*, *28*). Physiological studies to experimentally test this question are not possible in normal human subjects. However, certain disease states permit a glimpse into the consequences of HSC loss on progenitors and may shed light on the role of HSCs in human blood synthesis under nontransplant conditions. In aplastic anemia (AA), HSCs are damaged, likely due to an autoimmune response, and are unable to contribute to ongoing hematopoiesis (*29*, *30*). This effect seems to be specific to HSCs, because all mature blood lineages are depressed in AA (*31*–*33*). We examined the progenitor hierarchy in three cases of AA by applying our sorting scheme (Fig. 6). Consistent with previous reports, the proportion of CD34$^+$ cells within the overall mononuclear cell (MNC) pool was significantly lower in AA compared with normal BM (0.1% versus 4.2%, $P < 0.0001$, t test) (Fig. 6B) (*31*, *32*). The CD34$^+$CD38$^-$ stem cell compartment in AA patients was more significantly depleted compared with the CD34$^+$CD38$^+$ progenitor compartment (Fig. 6A, left column, and Fig. 6, C and D). Moreover, HSCs and MPPs were virtually undetectable in the residual CD34$^+$CD38$^-$ compartment, confirming that HSCs are specifically lost in this clinical condition (Fig. 6A, column 2), at least at the phenotypic level. Despite the loss of phenotypic HSCs, the CD34$^+$CD38$^+$ compartment was detectable in all cases. We quantified the subsets within the CD34$^+$CD38$^+$ compartment to determine whether all cell types are indiscriminately affected. Based on our single-cell functional readouts, we grouped progenitors enriched for myeloid (CMP F1, MEP F1, and GMP) and erythroid (CMP F2/F3 and MEP F2/F3) differentiation potential to increase the power of the analysis due to relative loss of CD34$^+$ cells in AA. Despite significant depletion of HSCs, the percentage of myeloid progenitors was stable compared with normal BM (Fig. 6E). In contrast, erythroid progenitors were significantly lost, like HSCs, in all three patients analyzed (Fig. 6F, $P < 0.0001$, t test). These results suggest that ongoing erythropoiesis is more reliant on HSC input compared with myelopoiesis. Although we cannot rule out a specific Er lineage defect in AA, the pan-lineage deficiencies observed in AA likely rule out this possibility and support the idea that the Er progenitor loss is most likely a repercussion of HSC depletion. Because all HSC types and MPPs seem to be broadly lost in AA, our results cannot distinguish which type of HSC is crucial to maintain erythropoiesis. Recognizing that hematopoiesis in AA is not normal, the revised hierarchy model predicted from our experimental data does appear to have physiological relevance in the human setting.

Discussion

Our study challenges the current view that human blood development occurs progressively through a series of multipotent, oligopotent, and then unilineage progenitor stages. By subjecting the classically defined progenitor subsets to a sorting scheme that efficiently resolved My, Er, and Mk lineage fates, combined with single-cell functional analysis, we made two findings. First, we found that the cellular hierarchy of human blood is not identical across development. In FL, oligopotent progenitors with My-Er-Mk and Er-Mk activity were a prominent component of the hierarchy. By contrast, the BM was dominated by unilineage progenitors with primarily My or Er potential. This shift in progenitor classes demarcates a fundamental readjustment in the blood hierarchy during in utero to adulthood time points. The absence of oligopotent intermediates that become gradually restricted to unilineage progenitors in BM cannot be reconciled under the standard model of blood differentiation. Instead, our data support a hierarchy composed mainly of two tiers in adults: a top tier that contains multipotent cells such as HSCs and MPPs, and a bottom tier composed of committed unipotent progenitors (Fig. 7). We cannot formally rule out the presence of a highly transient adult CMP-like progenitor stage that exists when multipotent cells differentiate into unipotent progenitors; however, our in vitro and in vivo assays surveyed large cell numbers (~3000), and such a progenitor was not detected. If lineage-restricted cell types able to generate a subset or full spectrum of myeloid cells do exist in the stem cell compartment of adult marrow, they most probably represent the murine counterparts of myeloid-biased or myeloid-restricted HSC subtypes (*7*, *34*). Second, we found the origins

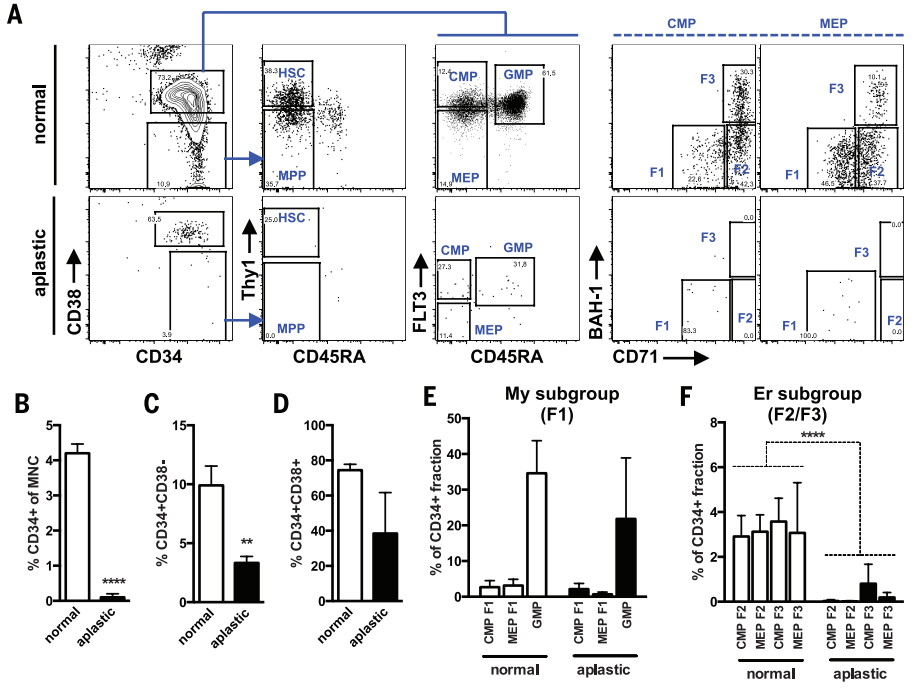

Fig. 6. Analysis of My and Er progenitors in patients with AA. (**A**) To examine the consequences of HSC loss on progenitor subsets, BM cells from three AA patients and normal controls were subjected to the new sorting design shown in Fig. 1B. Representative flow plots from a single AA case and a control are shown. (**B**) Quantification of total CD34$^+$ cells as a fraction of MNC pool from controls (empty bars) versus AA (filled bars). (**C** and **D**) The CD34$^+$ subset from controls and AA was further subdivided into the stem (CD34$^+$CD38$^-$) and progenitor (CD34$^+$CD38$^+$) cell compartments. (**E**) Analysis of My-enriched subsets (CMP F1, MEP F1, and GMP) in controls and in AA. (**F**) Analysis of Er-enriched subsets (CMP F2/F3 and MEP F2/F3) in controls and in AA. Bars indicate mean ± SE from three controls and three cases of AA. Asterisks indicate significance based on t test (**$P < 0.01$, ****$P < 0.0001$).

of the Mk lineage branch change from FL to BM. In FL, Mk progenitors were enriched but not restricted to the stem cell compartment, whereas in BM, the Mk lineage was closely tied to the fate of multipotent cells. These data are not consistent with the principal tenet of the standard model that My, Er, and Mk lineages originate from a common lineage progenitor such as CMP.

Historically, the first major lineage bifurcation step in the blood hierarchy was considered to be the segregation of myeloid (My-Er-Mk) and lymphoid fates (B, T, or Nk), with CMPs occupying the lineage fork that gives rise to the entire myeloid arm. The coemergence of My, Er, and Mk lineages was central to the description of CMPs. Our results reveal that the originally defined CMPs are highly heterogeneous, primarily composed of unipotent My or Er progenitors, with little Mk activity. In the absence of CMPs, how can the origins of lineage-restricted progenitors such as GMPs and MEPs be reconciled? Our previous clonal analysis suggested that myelomonocytic lineages originate from MLPs, which we suspect are the most probable precursor of GMPs, owing to their shared functional and transcriptional profiles (*11*, *12*, *35*). In this study, we found that *GATA-1*–positive Mk-Er–committed progenitors exist in the stem cell compartment, suggesting that MEPs are derived from multipotent cells. In the murine bone marrow niche, up to a quarter of LT-HSCs lie directly adjacent to Mks (*36*–*38*). Mks play a dual role in HSC regulation. Under normal conditions, Mk-HSC contact is essential to preserve the quiescent nature of adult LT-HSCs. After myeloablation, this effect is temporarily abrogated and Mks secrete growth factors that permit HSCs to expand (*37*). Thus, direct differentiation of Mks from HSCs may represent a physical mechanism to regulate blood stem cell functionality in the niche. Overall, the first major bifurcation step in blood differentiation is far more complex than a simple segregation of myeloid and lymphoid lineages. In humans, we suspect that this first step splits the Mk-Er lineage from the myelomonocytic lineage that cosegregates with the lymphoid fate (*11*). Why the myelomonocytic lineage, but not the granulocytic lineage, is tied to the lymphoid fate will be a critical area of future investigation (*39*, *40*). The ability to isolate developmental populations reported here provides a critical experimental framework to facilitate such studies in humans.

Our data may also have implications for our understanding of lineage specification at the molecular level. *vWF*, a key molecular marker strongly associated with Mk differentiation, was expressed in a subset of BM HSCs and may identify an HSC subtype primed for platelet production as shown in mouse (*16*). Molecular factors involved in Mk (*vWF*), Er (*EPOR*), and My (*CSF2RA*) differentiation were expressed in small pockets of single cells from undifferentiated cells, like BM HSCs, in a near mutually exclusive manner. This is consistent with the notion that transcription factors (TFs) associated with myeloid lineage specification are individually but not simultaneously primed at the level of stem cells. It is difficult to preclude that this type of molecular heterogeneity reflects impurities in human HSC isolation. However, analysis of purer murine HSC compartments supports that molecular factors associated with lineage commitment are stochastically activated at the level of HSCs (*16*, *17*). Maintenance of a multipotent state is thought to occur via low-level lineage priming, where TFs of different lineages are coexpressed in the same cell. In this model, commitment toward a particular lineage occurs by the mutual antagonism of these TFs, where one TF eventually wins, locking in a differentiation program. However, the near mutually exclusive expression of *vWF*, *CSFR2A*, and *EPOR* in BM HSCs does not agree with this logic. The hypothesis that lineage commitment occurs in the absence of a coordinated differentiation program (*17*, *25*, *41*) is more consistent with our data.

Ultimately, a better understanding of normal blood differentiation programs will be critical to deciphering how such programs go awry in disease. Indeed, in AA, we observed that Mk-Er progenitors are lost alongside HSC, but the My progenitor pool can continue to persist. Recent evidence from murine in situ tracking expriments showed that My progenitors can be sustained long term without contribution from HSCs (*27*, *28*). If human My progenitors are similarly long-lived, they would have a higher probability of acquiring mutations that could lead to clonal expansion and eventual My lineage leukemias. The short-lived nature of Mk-Er progenitors and their dependency on HSC input reduce their probability of accumulating enough mutations leading to leukemia. Clinical evidence that acute leukemia of the Mk and Er lineages is extremely rare compared with My leukemia is consistent with this idea. Our work on AA highlights one example of the clinical utility of a high-resolution developmental road map of normal hematopoiesis. The adaptable nature of our new sorting scheme should similarly inform on other hematological conditions.

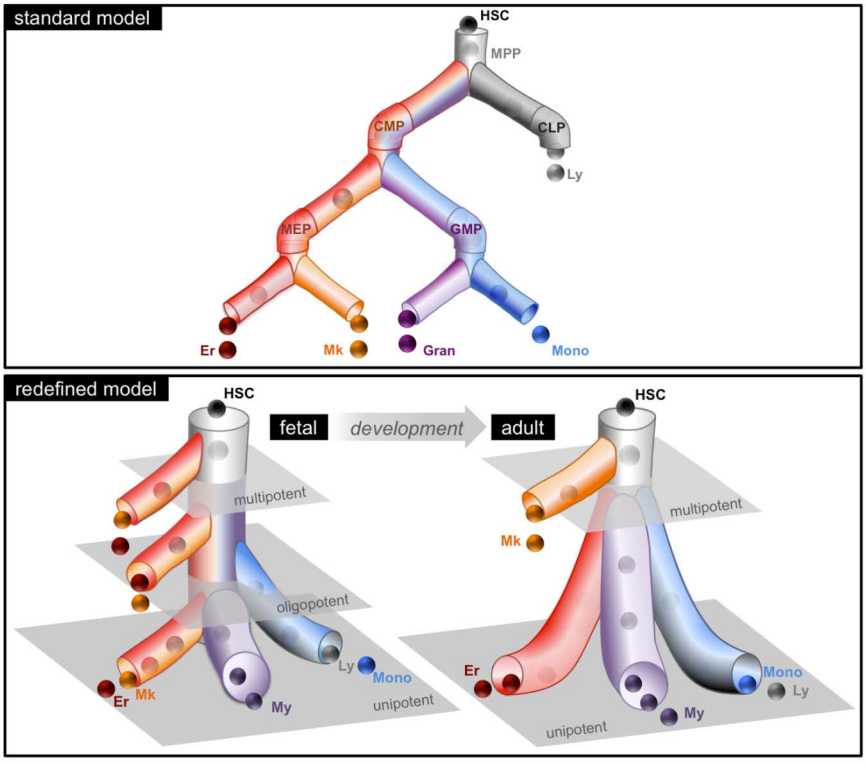

Fig. 7. A model of the changes in human My-Er-Mk differentiation that occur across developmental time points. Graphical depiction of My-Er-Mk cell differentiation that encompasses the predominant lineage potential of progenitor subsets; the standard model is shown for comparison. The redefined model proposes a developmental shift in the progenitor cell architecture from the fetus, where many stem and progenitor cell types are multipotent, to the adult, where the stem cell compartment is multipotent but the progenitors are unipotent. The grayed planes represent theoretical tiers of differentiation.

REFERENCES AND NOTES

1. J. E. Till, E. A. McCulloch, Hemopoietic stem cell differentiation. *Biochim. Biophys. Acta* **605**, 431–459 (1980). pmid: 7006701
2. G. J. Spangrude *et al.*, Mouse hematopoietic stem cells. *Blood* **78**, 1395–1402 (1991). pmid: 1884012
3. K. Akashi, D. Traver, T. Miyamoto, I. L. Weissman, A clonogenic common myeloid progenitor that gives rise to all myeloid lineages. *Nature* **404**, 193–197 (2000). doi: 10.1038/35004599; pmid: 10724173
4. M. Kondo, I. L. Weissman, K. Akashi, Identification of clonogenic common lymphoid progenitors in mouse bone marrow. *Cell* **91**, 661–672 (1997). doi: 10.1016/S0092-8674(00)80453-5; pmid: 9393859
5. J. Adolfsson *et al.*, Identification of Flt3$^+$ lympho-myeloid stem cells lacking erythro-megakaryocytic potential a revised road map for adult blood lineage commitment. *Cell* **121**, 295–306 (2005). doi: 10.1016/j.cell.2005.02.013; pmid: 15851035
6. R. Månsson *et al.*, Molecular evidence for hierarchical transcriptional lineage priming in fetal and adult stem cells and

multipotent progenitors. *Immunity* **26**, 407–419 (2007). doi: 10.1016/j.immuni.2007.02.013; pmid: 17433729
7. R. Yamamoto *et al*., Clonal analysis unveils self-renewing lineage-restricted progenitors generated directly from hematopoietic stem cells. *Cell* **154**, 1112–1126 (2013). doi: 10.1016/j.cell.2013.08.007; pmid: 23993099
8. S. Doulatov, F. Notta, E. Laurenti, J. E. Dick, Hematopoiesis: A human perspective. *Cell Stem Cell* **10**, 120–136 (2012). doi: 10.1016/j.stem.2012.01.006; pmid: 22305562
9. M. G. Manz, T. Miyamoto, K. Akashi, I. L. Weissman, Prospective isolation of human clonogenic common myeloid progenitors. *Proc. Natl. Acad. Sci. U.S.A.* **99**, 11872–11877 (2002). doi: 10.1073/pnas.172384399; pmid: 12193648
10. A. Galy, M. Travis, D. Cen, B. Chen, Human T, B, Natural killer, and dendritic cells arise from a common bone marrow progenitor cell subset. *Immunity* **3**, 459–473 (1995). doi: 10.1016/1074-7613(95)90175-2; pmid: 7584137
11. S. Doulatov *et al*., Revised map of the human progenitor hierarchy shows the origin of macrophages and dendritic cells in early lymphoid development. *Nat. Immunol.* **11**, 585–593 (2010). doi: 10.1038/ni.1889; pmid: 20543838
12. E. Laurenti *et al*., The transcriptional architecture of early human hematopoiesis identifies multilevel control of lymphoid commitment. *Nat. Immunol.* **14**, 756–763 (2013). doi: 10.1038/ni.2615; pmid: 23708252
13. C. J. H. Pronk *et al*., Elucidation of the phenotypic, functional, and molecular topography of a myeloerythroid progenitor cell hierarchy. *Cell Stem Cell* **1**, 428–442 (2007). doi: 10.1016/j.stem.2007.07.005; pmid: 18371379
14. G. Guo *et al*., Mapping cellular hierarchy by single-cell analysis of the cell surface repertoire. *Cell Stem Cell* **13**, 492–505 (2013). doi: 10.1016/j.stem.2013.07.017; pmid: 24035353
15. S. H. Naik *et al*., Diverse and heritable lineage imprinting of early haematopoietic progenitors. *Nature* **496**, 229–232 (2013). doi: 10.1038/nature12013; pmid: 23552896
16. A. Sanjuan-Pla *et al*., Platelet-biased stem cells reside at the apex of the haematopoietic stem-cell hierarchy. *Nature* **502**, 232–236 (2013). doi: 10.1038/nature12495; pmid: 23934107
17. C. Pina *et al*., Inferring rules of lineage commitment in haematopoiesis. *Nat. Cell Biol.* **14**, 287–294 (2012). doi: 10.1038/ncb2442; pmid: 22344032
18. F. Notta *et al*., Isolation of single human hematopoietic stem cells capable of long-term multilineage engraftment. *Science* **333**, 218–221 (2011). doi: 10.1126/science.1201219; pmid: 21737740
19. H. Qian *et al*., Critical role of thrombopoietin in maintaining adult quiescent hematopoietic stem cells. *Cell Stem Cell* **1**, 671–684 (2007). doi: 10.1016/j.stem.2007.10.008; pmid: 18371408
20. G. P. Solar *et al*., Role of c-mpl in early hematopoiesis. *Blood* **92**, 4–10 (1998). pmid: 9639492
21. B. Deng *et al*., An agonist murine monoclonal antibody to the human c-Mpl receptor stimulates megakaryocytopoiesis. *Blood* **92**, 1981–1988 (1998). pmid: 9731056
22. L. Edvardsson, J. Dykes, T. Olofsson, Isolation and characterization of human myeloid progenitor populations—TpoR as discriminator between common myeloid and megakaryocyte/erythroid progenitors. *Exp. Hematol.* **34**, 599–609 (2006). doi: 10.1016/j.exphem.2006.01.017; pmid: 16647566
23. L. A. Kohn *et al*., Lymphoid priming in human bone marrow begins before expression of CD10 with upregulation of L-selectin. *Nat. Immunol.* **13**, 963–971 (2012). doi: 10.1038/ni.2405; pmid: 22941246
24. F. Mazurier, M. Doedens, O. I. Gan, J. E. Dick, Rapid myeloerythroid repopulation after intrafemoral transplantation of NOD-SCID mice reveals a new class of human stem cells. *Nat. Med.* **9**, 959–963 (2003). doi: 10.1038/nm886; pmid: 12796774
25. T. Enver, M. Pera, C. Peterson, P. W. Andrews, Stem cell states, fates, and the rules of attraction. *Cell Stem Cell* **4**, 387–397 (2009). doi: 10.1016/j.stem.2009.04.011; pmid: 19427289
26. D. Ramsköld *et al*., Full-length mRNA-Seq from single-cell levels of RNA and individual circulating tumor cells. *Nat. Biotechnol.* **30**, 777–782 (2012). doi: 10.1038/nbt.2282; pmid: 22820318
27. J. Sun *et al*., Clonal dynamics of native haematopoiesis. *Nature* **514**, 322–327 (2014). doi: 10.1038/nature13824; pmid: 25296256
28. K. Busch *et al*., Fundamental properties of unperturbed haematopoiesis from stem cells in vivo. *Nature* **518**, 542–546 (2015). doi: 10.1038/nature14242; pmid: 25686605
29. V. G. Sankaran, M. J. Weiss, Anemia: Progress in molecular mechanisms and therapies. *Nat. Med.* **21**, 221–230 (2015). doi: 10.1038/nm.3814; pmid: 25742458
30. J. P. Maciejewski, A. Risitano, Hematopoietic stem cells in aplastic anemia. *Arch. Med. Res.* **34**, 520–527 (2003). doi: 10.1016/j.arcmed.2003.09.009; pmid: 14734092
31. J. C. Marsh, J. Chang, N. G. Testa, J. M. Hows, T. M. Dexter, The hematopoietic defect in aplastic anemia assessed by long-term marrow culture. *Blood* **76**, 1748–1757 (1990). pmid: 2224124
32. S. Rizzo *et al*., Stem cell defect in aplastic anemia: Reduced long term culture-initiating cells (LTC-IC) in $CD34^+$ cells isolated from aplastic anemia patient bone marrow. *Hematol. J.* **3**, 230–236 (2002). doi: 10.1038/sj.thj.6200187; pmid: 12391540
33. W. H. Matsui, R. A. Brodsky, B. D. Smith, M. J. Borowitz, R. J. Jones, Quantitative analysis of bone marrow CD34 cells in aplastic anemia and hypoplastic myelodysplastic syndromes. *Leukemia* **20**, 458–462 (2006). doi: 10.1038/sj.leu.2404119; pmid: 16437138
34. C. Benz *et al*., Hematopoietic stem cell subtypes expand differentially during development and display distinct lymphopoietic programs. *Cell Stem Cell* **10**, 273–283 (2012). doi: 10.1016/j.stem.2012.02.007; pmid: 22385655
35. T. Yoshida, S. Y.-M. Ng, J.-C. Zuñiga-Pflucker, K. Georgopoulos, Early hematopoietic lineage restrictions directed by Ikaros. *Nat. Immunol.* **7**, 382–391 (2006). doi: 10.1038/ni1314; pmid: 16518393
36. S. Y. Heazlewood *et al*., Megakaryocytes co-localise with hemopoietic stem cells and release cytokines that up-regulate stem cell proliferation. *Stem Cell Res.* **11**, 782–792 (2013). doi: 10.1016/j.scr.2013.05.007; pmid: 23792434
37. M. Zhao *et al*., Megakaryocytes maintain homeostatic quiescence and promote post-injury regeneration of hematopoietic stem cells. *Nat. Med.* **20**, 1321–1326 (2014). doi: 10.1038/nm.3706; pmid: 25326798
38. I. Bruns *et al*., Megakaryocytes regulate hematopoietic stem cell quiescence through CXCL4 secretion. *Nat. Med.* **20**, 1315–1320 (2014). doi: 10.1038/nm.3707; pmid: 25326802
39. A. Görgens *et al*., Revision of the human hematopoietic tree: Granulocyte subtypes derive from distinct hematopoietic lineages. *Cell Reports* **3**, 1539–1552 (2013). doi: 10.1016/j.celrep.2013.04.025; pmid: 23707063
40. Y. Mori *et al*., Identification of the human eosinophil lineage-committed progenitor: Revision of phenotypic definition of the human common myeloid progenitor. *J. Exp. Med.* **206**, 183–193 (2009). doi: 10.1084/jem.20081756; pmid: 19114669
41. M. A. Rieger, P. S. Hoppe, B. M. Smejkal, A. C. Eitelhuber, T. Schroeder, Hematopoietic cytokines can instruct lineage choice. *Science* **325**, 217–218 (2009). doi: 10.1126/science.1171461; pmid: 19590005

ACKNOWLEDGMENTS

We thank all members of the Dick laboratory for critical review of the manuscript, especially J. C. Y. Wang, E. Lechman, and M. Cooper; and N. Simard and S. Zhao and members of the Sickkids-UHN Flow Cytometry facility for technical support. We thank K. Moore and the obstetrics unit of Trillium Hospital (Mississauga, Ontario) for providing cord blood. We thank J. Rohrer from BD Biosciences (La Jolla, CA) for supplying BAH-1 clone. This work was supported by postdoctoral fellowship awards from the Canadian Institute of Health Research (CIHR) to F.N. and S.Z. S.Z. is supported by the Aplastic Anemia and Myelodysplasia Association of Canada. F.N. is a recipient of a scholar's research award from the Ontario Institute of Cancer Research (OICR), through generous support from the Ontario Ministry of Research and Innovation. Research in E.L.'s laboratory is supported by a Wellcome Trust Sir Henry Dale Fellowship and a core support grant from the Wellcome Trust and the Medical Research Council to the Wellcome Trust–Medical Research Council Cambridge Stem Cell Institute. Work in the Dick laboratory is supported by grants from CIHR, Canadian Cancer Society, Terry Fox Foundation, Genome Canada through the Ontario Genomics Institute, OICR with funds from the province of Ontario, a Canada Research Chair, and the Ontario Ministry of Health and Long-Term Care (OMOHLTC). Author Contributions: F.N., S.Z., and J.E.D. designed the study; F.N. and S.Z. analyzed and interpreted data; F.N., S.Z., N.T., S.D., O.I.G., and J.M. performed experiments; G.W., J.D.M., and L.D.S. performed RNA sequencing and analysis. K.B.K., S.Z., F.N., and J.E.D. generated the model; Y.D. provided clinical samples from aplastic anemia and matched controls for the study. F.N., S.Z., and J.E.D. wrote the manuscript; all authors reviewed and approved the manuscript; J.E.D. supervised the study. Aplastic anemia samples are available from Y.D. under a material transfer agreement with Toronto Sickkids Hospital. Gene expression data have been submitted to the Gene Expression Omnibus (no. GSE76234).

SUPPLEMENTARY MATERIALS

www.sciencemag.org/content/351/6269/aab2116/suppl/DC1
Materials and Methods
Supplementary Text
Figs. S1 to S7
Table S1
References (*42*–*44*)

26 March 2015; accepted 23 October 2015
Published online 5 November 2015
10.1126/science.aab2116

Distinct routes of lineage development reshape the human blood hierarchy across ontogeny

Faiyaz Notta, Sasan Zandi, Naoya Takayama, Stephanie Dobson, Olga I. Gan, Gavin Wilson, Kerstin B. Kaufmann, Jessica McLeod, Elisa Laurenti, Cyrille F. Dunant, John D. McPherson, Lincoln D. Stein, Yigal Dror and John E. Dick

Science **351** (6269), aab2116.
DOI: 10.1126/science.aab2116originally published online November 5, 2015

Adjusting hematopoietic hierarchy

In adults, more than 300 billion blood cells are replenished daily. This output arises from a cellular hierarchy where stem cells differentiate into a series of multilineage progenitors, culminating in unilineage progenitors that generate over 10 different mature blood cell types. Notta *et al.* mapped the lineage potential of nearly 3000 single cells from 33 different cell populations of stem and progenitor cells from fetal liver, cord blood, and adult bone marrow (see the Perspective by Cabezas-Wallscheid and Trumpp). Prenatally, stem cell and progenitor populations were multilineage with few unilineage progenitors. In adults, multilineage cell potential was only seen in stem cell populations.

Science, this issue p. 10.1126/science.aab2116; see also p. 126

www.sciencemag.org/cgi/content/full/science.aab2116/DC1

Supplementary Materials for

Distinct routes of lineage development reshape the human blood hierarchy across ontogeny

Faiyaz Notta, Sasan Zandi, Naoya Takayama, Stephanie Dobson, Olga I. Gan, Gavin Wilson, Kerstin B. Kaufmann, Jessica McLeod, Elisa Laurenti, Cyrille F. Dunant, John D. McPherson, Lincoln D. Stein, Yigal Dror, John E. Dick*

*Corresponding author. E-mail: jdick@uhnres.utoronto.ca

Published 5 November 2015 on *Science* Express
DOI: 10.1126/science.aab2116

This PDF file includes:

TABLE OF CONTENTS

Supplementary Text

Colony assays resolve phenotypic heterogeneity within newly defined subpopulations of human myeloid progenitors

The unexpected cellular heterogeneity that we uncovered prompted us to determine whether these progenitor fractions also exhibited functional heterogeneity. We first applied standard methylcellulose (MC) colony assays to our newly defined cell populations. Median cloning efficiency across all subsets was 38% in FL, 46% in CB and 36% in BM (fig. S3 A-B). CD49f+ HSC derived colonies were exclusively myeloid of which nearly half were of high proliferative potential (CFU-HPP; fig. S3B), reflecting their stem cell potential. The percentage of CFU-HPP gradually decreased in HSC compartments of FL, CB and BM (CFU-HPP: FL - 38%, CB - 31%, BM - 22%; Fig. S4B left). These data indicate that CD49f uniformly enriches HSCs across development, and is consistent with ongoing in vivo studies (SZ, NT, FN, JED unpublished). HPP colonies persisted at the MPP stage (CFU-HPP: FL – 6%, CB – 7%, BM – 3%; fig. S4B middle), and surprisingly FL and CB CMP F1 cells still produced rare HPP colonies (CFU-HPP; FL: 4%, CB: 7%, BM: 0%; fig. S4B right). In BM, no subset within CD34+CD38+ population carried HPP potential. In general, FL colonies often generated 10.5 larger colonies compared to BM irrespective of the subset analyzed (fig. S4B). These results complement the work of Lansdorp et al. performed two decades ago with bulk CD34+ cells from FL, CB and BM (*42*). We extend these findings and establish that proliferative changes in development are not only restricted to the stem cell compartment, but occur at all hierarchical levels.

The spectrum of lineage colonies was consistent across phenotypically matched subsets in FL, CB and BM (fig. S2A), and advocate that segregation of cellular subsets based on functional surface markers is able to stably discriminate comparable progenitors in development. Subsets defined by absence of CD71 and BAH-1 such as HSCs and F1 subsets of MPPs, CMPs and MEPs were highly enriched for CFU-My activity (fig. S3A). We reasoned that the absence of lineage commitment markers in the CMP compartment (CMP F1) would identify true human CMPs. However, greater than 70% of colonies from FL and CB CMP F1 were My only, and the rest were BFU-E (fig. S3A). In BM, CMP F1 cells were exclusively My (CFU-My, FL: 70%, CB: 76%, BM: 99%; fig. S3A). The increased proportion of CFU-My in BM correlates well with increased myelopoiesis observed in aging (*43*). These data propose that previously defined

CMPs consist mostly of unilineage My and Er progenitors. Although resolving Er progenitors with CD71 was expected, we found that BFU-E derived from MPP F2/3 were often larger than analogous F2/3s defined in the CMPs and MEPs (fig. S4A). This indicates that Er progenitors derived from CD34+CD38- versus CD34+CD38+ are functionally distinct.

Mk activity predominates in CD34+CD38- stem cell enriched compartment

Human Mk progenitors are poorly defined in the CD34+ hierarchy. The shortcomings of previous studies were partly due to use of standard colony assays, which rely on morphological based assessment for Mks. Alternate cytokine requirements of Mk indicate standard colony assays do not efficiently support differentiation along this lineage. We employed the highly specific collagen-based Megacult^{TM} assay that detects colony-forming unit-megakaryocyte (CFU-Mk) based on GPIIb/IIIa (CD41) staining (fig S3C-D). Using this assay, we found a striking enrichment of CFU-Mk in the CD34+CD38- stem cell compartment (fig. S3C). Of the 11 subsets we fractionated from FL, CB and BM, MPP F2 was particularly enriched for CFU-Mk potential (figs S3C). Although CFU-Mk activity was found in the CD34+CD38+ progenitor compartment, it was minimal in comparison (fig. S3C). Particularly important was the finding that MEP fractions were not strikingly enriched for CFU-Mk activity (fig. S3C). These results were consistent across FL, CB and BM. It was clear that the bulk of Mk potential resides within the CD34+CD38- compartment across development, rather than in the tradition view of MEP only arising from CMP. In conjunction with MC colony data that demonstrated concurrent enrichment for BFU-E from these subsets, it is formally possible that true MEPs reside within the stem cell compartment and not within classically defined MEPs within the CD34+CD38+ progenitor compartment. But absolute evidence that both Mk and Er colonies are derived from a common progenitor required single cell analysis.

Single cell transcription profiling of newly identified populations

Virtually, all single cells from CMP F1 and GMPs expressed at least one of three myeloid lineage factors such as *CEBPα*, *MPO* and *CSF2RA* (Fig. 5A) *CEBPα* is a master regulator of steady state myelopoiesis and activates the promoter of several critical myeloid genes to lock down myeloid development. Approximately 10% of FL and BM CMP F1 cells expressed *CEBPα* alongside *GATA1* or *EPOR*, suggesting molecular factors of My and Er fates co-exist in

some cells within CMP F1 (Fig. 5A). This coincides with the small percentage of mixed colony potential from this subset in the single cell assay (Fig. 3B). 20% of BM CMP F1 also co-expressed CEBPα with *EPOR* or *GATA1*. However unlike FL, BM CMP F1 cells did not co-express *EPOR* and *GATA1*. Moreover the expression of *CEBPα* and *MPO* was dramatically higher in BM CMP F1 suggesting a dominant My program is already established in CMP F1 cells that co-express My and Er factors (Fig 5A). Dramatically higher levels of *EPO* or *GATA1* observed in fully committed erythroid committed subsets, such as MEP F3 suggests the established E/Mk program that is also supported by the single cell functional assay (Fig. 5A).

Experimental Procedures

Human CD34+ Cord Blood, Bone Marrow, and Fetal Liver

Human cord blood samples were obtained from Trillium Hospital (Mississauga, Ontario, Canada with informed consent in accordance to guidelines approved by University Health Network (UHN) Research Ethics Board. Cord blood was processed 24 – 48h post-delivery. Mononuclear cells were enriched using Ficoll-Paque (GE Healthcare Life Sciences, cat. no. 17-1440-02) followed by red-blood lysis by ammonium chloride (Stemcell Technologies, cat. no. 07850). CD34+ selection was performed using CD34 Microbead kit (Miltenyi Biotech, cat. no. 130-046-703). Cells were viably stored at -80^{o}C or -150^{o}C. In most cases, individual donors were processed for experiments. CD34+ adult bone marrow was purchased from Lonza (cat. no. 2M-101C). Only bone marrow obtained from donors between 25 and 35 years of age were used in this study. CD34+ human fetal liver cells were purchased from AllCells (AllCells LLC, Alameda, CA, US, cat. no. FL-CD34-001F or FL-CD34-002F/~20-22wk gestation).

Cell Sorting

Viable cells were thawed via dropwise addition of IMDM based (IMDM + 20% fetal calf serum (FCS) + DNaseI). Final concentration of DNase I (Roche Applied Science, 10104159001) in IMDM solution was 200ug/mL. Post-thaw, cells were spun at low RPM (~1000) for 20min at 4^{o}C. After the spin, thawing solution was removed and cells were resuspended in 100uL of

PBS+5% FCS for exposure to antibodies. The following antibodies were used for cell sorting: CD7 PB (BD bioscience, clone M-T701), CD10 A700 (BD bioscience, clone HI10a, custom conjugation), CD34 APC-Cy7 (BD bioscience, clone 581, custom conjugation), CD38 PC7 (BD bioscience, clone HB7, cat. no. 335790), CD110(cMPL) PE (BD bioscience, clone BAH-1, custom conjugation), CD71 NC650 (ebioscience, clone OKT9, custom conjugation), CD135(FLT3) biotin (BD bioscience, clone 4G8, custom conjugation), CD45RA FITC (BD bioscience, clone HI100, cat. no. 555488), Thy1/CD90 APC (BD bioscience, clone 5E10, cat. no. 559869), CD49f PE-Cy5 BD bioscience, clone GoH3, cat. no. 551129), CD19 PE (BD bioscience, clone SJ25C1, cat. no. 340364), Strepavidin Qdot605 conjugate (Life Technologies, cat. no. Q10101MP). Cell sorting was performed on the BD FACSAria III.

Methylcellulose and MegaCult™ Assay

Cell populations were sorted directly into complete methylcellulose (cytokines: SCF, GM-CSF, IL-3, G-CSF, EPO; cat. no. H4034, Stem cell technologies). Complete methylcellulose medium was additionally supplemented with FLT3 ligand (20ng/mL final concentration), IL-6 (50ng/mL final concentration), LDL (4ug/mL final concentration, cat. no. 02698, Stem cell technologies). 300 cells were deposited by cell sorting into 3mL of methylcellulose, mixed and 1mL (100 cells) was plated into 35 mm dishes in duplicates. Colonies were allowed to differentiate for 14 days and were morphologically assessed for colonies. In the case for fetal liver, colonies were often picked and analyzed for flow cytometry as BFU-E did not hemoglobinize well. For cell counting, plates were resuspended in PBS/FCS and subsequently counted on the Vi-cell XR (Beckman Coulter). For Megacult, 200 sorted cells in technical duplicates were plated in a collagen-based material in double chamber culture slides and cultured for 10 days (MegaCult®-C Medium with Cytokines, Cat no: 04901/04951, Stem cell technologies). Staining for GPIIb/IIIa antibody and scoring of CFU-Mk colonies were performed according to manufacturer's protocol.

Single cell Assay

MS-5 stroma (kindly provided by Dr. K. Itoh, Japan) was seeded into 96-well flat bottom plates (Nunc) at a density of $3x10^3$ to $5x10^3$ cells in Myelocult medium (H5100, Stem cell

technologies) per well. MS-5 cells were seed in 100uL of medium an allowed to adhere for 24-48h prior to cell sorting. Before cell sorting, media was removed with multichannel pipet and 200uL of serum free media (StemPro34 SFM with nutrient, cat. no. 10639, Life Technologies) supplemented with (SCF – 100ng/mL, FLT3 – 20ng/mL, TPO – 100ng/mL, EPO – 3units/mL, IL-6 – 50ng/mL, IL-3 – 10ng/mL, IL-11 – 50ng/mL, GM-CSF – 20ng/mL, LDL – 4ug/mL, 2-ME, L-Glutamine, Pen-strep). Single cells were cultured for 2 weeks without media change. For HSC fraction, where some clones did not emerge till after 2 weeks, a half media change was performed. Wells content was harvested and subjected to flow cytometry for analysis (LSRII, BD biosciences). The following antibodies were used to assess myeloid cell lineages: (CD15 PB [clone MMA, cat. no. 642917, BD Biosciences], CD45 FITC [BD Biosciences, clone 2D1], GlyA PE [clone 11E4B-7-6, cat. no. IM2211U, Beckman Coulter], CD41 PC5 [clone P2, cat. no. PN 6607116, Beckman Coulter], CD14 PC7 [clone RM052, cat. no. A22331, Beckman Coulter], CD42b APC [clone HIP1, cat. no. 551061, BD Biosciences], CD11b APC7 [clone xxx, cat. no. xx, BD Biosciences]). Generally, greater than 10 cells were required to call a positive colony.

Fluidigm Assay and RNA sequencing

For RNA sequencing, HSC and progenitor subsets from CB were sorted (2000-4000 cells) and RNA was isolated using the mirVana RNA isolation kit (Ambion). RNA was subjected to amplification using SMARTer^{TM} Ultra Low RNA Kit for Illumina Sequencing (Clontech, Cat. No. 634826). Library preparation of cDNA was performed using the Nextera protocol (Illumina, Nextera DNA Sample Preparation Kit, Cat No. FC-121-1031). Each population was subjected to at least half lane of sequencing on Illumina HiSeq2000.

For the fluidigm protocol, single cells were sorted into eppendorf 96 well skirted plates with 5ul of cell lysis buffer containing 10% NP40 (Fisher Scientific, Cat# 28324), RNaseOut (life technology, Cat# 10777-019) and 5x VILO reaction mix (LT, Cat# 11754-050). To make cDNA from single cells, 0.15ul of 10x Supermix VILO (LT, Cat# 11754-050) and 0.12ul T4 Gene 32 protein (NEB,cat# M0300S) added to the mix and incubated in 25ºC, 5min; 50ºC, 30min; 55ºC, 25min; 60ºC, 5min and 70ºC 10min. TaqMan preamp Master Mix (life technology, Cat# 4391128) and up to 48 multiplexed inventoried TaqMan assays (final dilution 0.05×) were used to amplify 48 target cDNA. The cDNA target primers used in this study are shown below.

Zero, 2, 4 and 8 cells were included as control. RT–PCR pre-amplification cycling conditions were: 20x(95°C, 5sec; 60°C, 4min). Amplified material then cleaned up using 1.2ul of Exo I 20U/ul and 0.6ul of Exo I (NEB, Cat#M0293S) for 30 min in 37ºC. cDNA diluted 5x with water or TE buffer. qPCR was done with the same inventoried TaqMan assays using Fluidigm 48.48 Gene expression Dynamic Arrays (Fluidigm) chips and read in BioMark HDsystem according to manufacturer protocol for single cell QPCR. The data were exported into Microsoft Excel for downstream analysis. Data were analyzed using modified SINGuLAR™ Analysis Toolset and pheatmap package used to generate heatmaps in R. We set the cutoff level for expression at Ct>28. Samples with low GAPDH and PGK1 expression (Ct higher than 20) were considered as outliers and excluded from the analysis.

Assay ID	Gene Name	Cat#	Inventoried
Hs99999903_m1	ACTB	4331182	yes
Hs00269972_s1	CEBPA	4331182	yes
Hs00538896_m1	CSF2RA	4331182	Yes
Hs00237052_m1	CXCR4	4331182	yes
Hs00395519_m1	EBF1	4351372	yes
Hs00181092_m1	EPOR	4331182	yes
Hs00174690_m1	FLT3	4331182	yes
Hs99999905_m1	GAPDH	4331182	yes
Hs01085823_m1	GATA1	4331182	yes
Hs01119304_m1	MPL	4351372	yes
Hs00924296_m1	MPO	4331182	yes
Hs00172003_m1	PAX5	4331182	yes
Hs99999906_m1	PGK1	4331182	yes
Hs01548149_m1	PU.1	4351372	yes
Hs01109452_m1	VWF	4351372	yes

In Vivo Analysis

Only CB cells were used for in vivo analysis due to the number of cells required to generate engraftment. CB populations were sorted, recounted and resuspended in a volume of 25 µL/mouse for transplant. Eight to twelve week old female NOD.Cg-*Prkdc*^{scid} *Il2rg*^{tm1Wjl}/SzJ (NSG) mice were sublethally irradiated at 225cGy, 12-24 hours prior to transplant (*44*). Intrafemoral injections were performed as previously described (*24*). Briefly, mice were anesthetized with isoflurane, the right knee was secured in a bent position and a 27 gauge needle was used to drill into the right femur. Cells were then injected using a 28.5 gauge ½ cc syringe. Following 2-4 weeks mice were euthanized by cervical dislocation and peripheral blood (PB), right femur (RF) and bone marrow (left and right tibias and left femur, BM) were collected. BM bones were crushed in 1mL of IMDM + 5% FBS using a 2 oz glass mortar and pestle (Fisher

Scientific). Crushed bones were subsequently washed with 20 mL of media, filtered through a 40 μM cell strainer (BD Falcon), centrifuged and the resulting marrow cells resuspended in 1mL of IMDM + 5% FBS. Cells from RF and BM were counted using Vicell XR (Beckman Coulter). PB was collected in tubes containing heparin (Sigma cat. no H3149-10KU) and lysed with ammonium chloride (StemCell Technologies) prior to antibody staining. Cell aliquots were stained in 96-well round bottom plates (BD Falcon) and the human grafts were analyzed by flow cytometry (LSRII Becton Dickinson) for RF/BM: 15 PB (BD biosciences, clone MMA, cat. no. 642917), 45 FITC (BD bioscience, clone 2D1, cat. no. 347463), 19 PE (BD biosciences, clone 4G7, cat. no. 349209), GlyA PE (Coulter, clone 11E4B-7-6, cat. no. IM2211U), 45 PC5 (Coulter, clone J.33, cat. no. IM2653U), 14 PC7 (Coulter, clone RM052, cat. no. A22331), 33 APC (BD biosciences, clone p67.6, cat.no. 340474), 71 APC (BD bioscience, clone M-A712, cat. no. 551374), 34 APC7 (BD bioscience, clone 581, custom conjugation) and PB: CD45 FITC (BD bioscience), CD19 PE (BD biosciences, clone 4G7, cat. no. 349209), CD45 PC5 (Coulter, clone J.33, cat. no. IM2653U), CD41 PC7 (Coulter, clone P2, cat. no. 6607115), CD42b PE or APC (BD biosciences, clone HIP1), CD3 APC (BD biosciences, clone UCHT1, cat. no. 555335), CD11b APC7 (BD biosciences, clone ICRF44, cat. no. 557754).

References

1. J. E. Till, E. A. McCulloch, Hemopoietic stem cell differentiation. *Biochim. Biophys. Acta* **605**, 431–459 (1980). Medline

2. G. J. Spangrude, L. Smith, N. Uchida, K. Ikuta, S. Heimfeld, J. Friedman, I. L. Weissman, Mouse hematopoietic stem cells. *Blood* **78**, 1395–1402 (1991). Medline

3. J. Adolfsson, R. Månsson, N. Buza-Vidas, A. Hultquist, K. Liuba, C. T. Jensen, D. Bryder, L. Yang, O. J. Borge, L. A. Thoren, K. Anderson, E. Sitnicka, Y. Sasaki, M. Sigvardsson, S. E. Jacobsen, Identification of Flt3+ lympho-myeloid stem cells lacking erythro-megakaryocytic potential a revised road map for adult blood lineage commitment. *Cell* **121**, 295–306 (2005). Medline doi:10.1016/j.cell.2005.02.013

4. R. Månsson, A. Hultquist, S. Luc, L. Yang, K. Anderson, S. Kharazi, S. Al-Hashmi, K. Liuba, L. Thorén, J. Adolfsson, N. Buza-Vidas, H. Qian, S. Soneji, T. Enver, M. Sigvardsson, S. E. Jacobsen, Molecular evidence for hierarchical transcriptional lineage priming in fetal and adult stem cells and multipotent progenitors. *Immunity* **26**, 407–419 (2007). Medline doi:10.1016/j.immuni.2007.02.013

5. R. Yamamoto, Y. Morita, J. Ooehara, S. Hamanaka, M. Onodera, K. L. Rudolph, H. Ema, H. Nakauchi, Clonal analysis unveils self-renewing lineage-restricted progenitors generated directly from hematopoietic stem cells. *Cell* **154**, 1112–1126 (2013). Medline doi:10.1016/j.cell.2013.08.007

6. S. Doulatov, F. Notta, E. Laurenti, J. E. Dick, Hematopoiesis: A human perspective. *Cell Stem Cell* **10**, 120–136 (2012). Medline doi:10.1016/j.stem.2012.01.006

7. K. Akashi, D. Traver, T. Miyamoto, I. L. Weissman, A clonogenic common myeloid progenitor that gives rise to all myeloid lineages. *Nature* **404**, 193–197 (2000). Medline doi:10.1038/35004599

8. M. Kondo, I. L. Weissman, K. Akashi, Identification of clonogenic common lymphoid progenitors in mouse bone marrow. *Cell* **91**, 661–672 (1997). Medline doi:10.1016/S0092-8674(00)80453-5

9. M. G. Manz, T. Miyamoto, K. Akashi, I. L. Weissman, Prospective isolation of human clonogenic common myeloid progenitors. *Proc. Natl. Acad. Sci. U.S.A.* **99**, 11872–11877 (2002). Medline doi:10.1073/pnas.172384399

10. A. Galy, M. Travis, D. Cen, B. Chen, Human T, B, natural killer, and dendritic cells arise from a common bone marrow progenitor cell subset. *Immunity* **3**, 459–473 (1995). Medline doi:10.1016/1074-7613(95)90175-2

11. S. Doulatov, F. Notta, K. Eppert, L. T. Nguyen, P. S. Ohashi, J. E. Dick, Revised map of the human progenitor hierarchy shows the origin of macrophages and dendritic cells in early lymphoid development. *Nat. Immunol.* **11**, 585–593 (2010). Medline doi:10.1038/ni.1889

12. E. Laurenti, S. Doulatov, S. Zandi, I. Plumb, J. Chen, C. April, J. B. Fan, J. E. Dick, The transcriptional architecture of early human hematopoiesis identifies multilevel control of lymphoid commitment. *Nat. Immunol.* **14**, 756–763 (2013). Medline doi:10.1038/ni.2615

13. C. J. H. Pronk, D. J. Rossi, R. Månsson, J. L. Attema, G. L. Norddahl, C. K. Chan, M. Sigvardsson, I. L. Weissman, D. Bryder, Elucidation of the phenotypic, functional, and molecular topography of a myeloerythroid progenitor cell hierarchy. *Cell Stem Cell* **1**, 428–442 (2007). Medline doi:10.1016/j.stem.2007.07.005

14. G. Guo, S. Luc, E. Marco, T. W. Lin, C. Peng, M. A. Kerenyi, S. Beyaz, W. Kim, J. Xu, P. P. Das, T. Neff, K. Zou, G. C. Yuan, S. H. Orkin, Mapping cellular hierarchy by single-cell analysis of the cell surface repertoire. *Cell Stem Cell* **13**, 492–505 (2013). Medline doi:10.1016/j.stem.2013.07.017

15. S. H. Naik, L. Perié, E. Swart, C. Gerlach, N. van Rooij, R. J. de Boer, T. N. Schumacher, Diverse and heritable lineage imprinting of early haematopoietic progenitors. *Nature* **496**, 229–232 (2013). Medline doi:10.1038/nature12013

16. A. Sanjuan-Pla, I. C. Macaulay, C. T. Jensen, P. S. Woll, T. C. Luis, A. Mead, S. Moore, C. Carella, S. Matsuoka, T. Bouriez Jones, O. Chowdhury, L. Stenson, M. Lutteropp, J. C. Green, R. Facchini, H. Boukarabila, A. Grover, A. Gambardella, S. Thongjuea, J. Carrelha, P. Tarrant, D. Atkinson, S. A. Clark, C. Nerlov, S. E. Jacobsen, Platelet-biased stem cells reside at the apex of the haematopoietic stem-cell hierarchy. *Nature* **502**, 232–236 (2013). Medline doi:10.1038/nature12495

17. C. Pina, C. Fugazza, A. J. Tipping, J. Brown, S. Soneji, J. Teles, C. Peterson, T. Enver, Inferring rules of lineage commitment in haematopoiesis. *Nat. Cell Biol.* **14**, 287–294 (2012). Medline doi:10.1038/ncb2442

18. F. Notta, S. Doulatov, E. Laurenti, A. Poeppl, I. Jurisica, J. E. Dick, Isolation of single human hematopoietic stem cells capable of long-term multilineage engraftment. *Science* **333**, 218–221 (2011). Medline doi:10.1126/science.1201219

19. H. Qian, N. Buza-Vidas, C. D. Hyland, C. T. Jensen, J. Antonchuk, R. Månsson, L. A. Thoren, M. Ekblom, W. S. Alexander, S. E. Jacobsen, Critical role of thrombopoietin in maintaining adult quiescent hematopoietic stem cells. *Cell Stem Cell* **1**, 671–684 (2007). Medline doi:10.1016/j.stem.2007.10.008

20. G. P. Solar, W. G. Kerr, F. C. Zeigler, D. Hess, C. Donahue, F. J. de Sauvage, D. L. Eaton, Role of c-mpl in early hematopoiesis. *Blood* **92**, 4–10 (1998). Medline

21. B. Deng, N. Banu, B. Malloy, P. Hass, J. F. Wang, L. Cavacini, D. Eaton, H. Avraham, An agonist murine monoclonal antibody to the human c-Mpl receptor stimulates megakaryocytopoiesis. *Blood* **92**, 1981–1988 (1998). Medline

22. L. Edvardsson, J. Dykes, T. Olofsson, Isolation and characterization of human myeloid progenitor populations—TpoR as discriminator between common myeloid and megakaryocyte/erythroid progenitors. *Exp. Hematol.* **34**, 599–609 (2006). Medline doi:10.1016/j.exphem.2006.01.017

23. L. A. Kohn, Q. L. Hao, R. Sasidharan, C. Parekh, S. Ge, Y. Zhu, H. K. Mikkola, G. M. Crooks, Lymphoid priming in human bone marrow begins before expression of CD10 with upregulation of L-selectin. *Nat. Immunol.* **13**, 963–971 (2012). Medline doi:10.1038/ni.2405

24. F. Mazurier, M. Doedens, O. I. Gan, J. E. Dick, Rapid myeloerythroid repopulation after intrafemoral transplantation of NOD-SCID mice reveals a new class of human stem cells. *Nat. Med.* **9**, 959–963 (2003). Medline doi:10.1038/nm886

25. T. Enver, M. Pera, C. Peterson, P. W. Andrews, Stem cell states, fates, and the rules of attraction. *Cell Stem Cell* **4**, 387–397 (2009). Medline doi:10.1016/j.stem.2009.04.011

26. D. Ramsköld, S. Luo, Y. C. Wang, R. Li, Q. Deng, O. R. Faridani, G. A. Daniels, I. Khrebtukova, J. F. Loring, L. C. Laurent, G. P. Schroth, R. Sandberg, Full-length mRNA-Seq from single-cell levels of RNA and individual circulating tumor cells. *Nat. Biotechnol.* **30**, 777–782 (2012). Medline doi:10.1038/nbt.2282

27. J. Sun, A. Ramos, B. Chapman, J. B. Johnnidis, L. Le, Y. J. Ho, A. Klein, O. Hofmann, F. D. Camargo, Clonal dynamics of native haematopoiesis. *Nature* **514**, 322–327 (2014). Medline doi:10.1038/nature13824

28. K. Busch, K. Klapproth, M. Barile, M. Flossdorf, T. Holland-Letz, S. M. Schlenner, M. Reth, T. Höfer, H. R. Rodewald, Fundamental properties of unperturbed haematopoiesis from stem cells in vivo. *Nature* **518**, 542–546 (2015). Medline doi:10.1038/nature14242

29. V. G. Sankaran, M. J. Weiss, Anemia: Progress in molecular mechanisms and therapies. *Nat. Med.* **21**, 221–230 (2015). Medline doi:10.1038/nm.3814

30. J. P. Maciejewski, A. Risitano, Hematopoietic stem cells in aplastic anemia. *Arch. Med. Res.* **34**, 520–527 (2003). Medline doi:10.1016/j.arcmed.2003.09.009

31. J. C. Marsh, J. Chang, N. G. Testa, J. M. Hows, T. M. Dexter, The hematopoietic defect in aplastic anemia assessed by long-term marrow culture. *Blood* **76**, 1748–1757 (1990). Medline

32. S. Rizzo, J. Scopes, M. O. Elebute, H. A. Papadaki, E. C. Gordon-Smith, F. M. Gibson, Stem cell defect in aplastic anemia: Reduced long term culture-initiating cells (LTC-IC) in CD34+ cells isolated from aplastic anemia patient bone marrow. *Hematol. J.* **3**, 230–236 (2002). Medline doi:10.1038/sj.thj.6200187

33. W. H. Matsui, R. A. Brodsky, B. D. Smith, M. J. Borowitz, R. J. Jones, Quantitative analysis of bone marrow CD34 cells in aplastic anemia and hypoplastic myelodysplastic syndromes. *Leukemia* **20**, 458–462 (2006). Medline doi:10.1038/sj.leu.2404119

34. C. Benz, M. R. Copley, D. G. Kent, S. Wohrer, A. Cortes, N. Aghaeepour, E. Ma, H. Mader, K. Rowe, C. Day, D. Treloar, R. R. Brinkman, C. J. Eaves, Hematopoietic stem cell subtypes expand differentially during development and display distinct lymphopoietic programs. *Cell Stem Cell* **10**, 273–283 (2012). Medline doi:10.1016/j.stem.2012.02.007

35. T. Yoshida, S. Y.-M. Ng, J.-C. Zuñiga-Pflucker, K. Georgopoulos, Early hematopoietic lineage restrictions directed by Ikaros. *Nat. Immunol.* **7**, 382–391 (2006). Medline doi:10.1038/ni1314

36. S. Y. Heazlewood, R. J. Neaves, B. Williams, D. N. Haylock, T. E. Adams, S. K. Nilsson, Megakaryocytes co-localise with hemopoietic stem cells and release cytokines that up-regulate stem cell proliferation. *Stem Cell Res.* **11**, 782–792 (2013). Medline doi:10.1016/j.scr.2013.05.007

37. M. Zhao, J. M. Perry, H. Marshall, A. Venkatraman, P. Qian, X. C. He, J. Ahamed, L. Li, Megakaryocytes maintain homeostatic quiescence and promote post-injury regeneration of hematopoietic stem cells. *Nat. Med.* **20**, 1321–1326 (2014). Medline doi:10.1038/nm.3706

38. I. Bruns, D. Lucas, S. Pinho, J. Ahmed, M. P. Lambert, Y. Kunisaki, C. Scheiermann, L. Schiff, M. Poncz, A. Bergman, P. S. Frenette, Megakaryocytes regulate hematopoietic stem cell quiescence through CXCL4 secretion. *Nat. Med.* **20**, 1315–1320 (2014). Medline doi:10.1038/nm.3707

39. A. Görgens, S. Radtke, M. Möllmann, M. Cross, J. Dürig, P. A. Horn, B. Giebel, Revision of the human hematopoietic tree: Granulocyte subtypes derive from distinct hematopoietic lineages. *Cell Reports* **3**, 1539–1552 (2013). Medline doi:10.1016/j.celrep.2013.04.025

40. Y. Mori, H. Iwasaki, K. Kohno, G. Yoshimoto, Y. Kikushige, A. Okeda, N. Uike, H. Niiro, K. Takenaka, K. Nagafuji, T. Miyamoto, M. Harada, K. Takatsu, K. Akashi, Identification of the human eosinophil lineage-committed progenitor: Revision of phenotypic definition of the human common myeloid progenitor. *J. Exp. Med.* **206**, 183–193 (2009). Medline doi:10.1084/jem.20081756

41. M. A. Rieger, P. S. Hoppe, B. M. Smejkal, A. C. Eitelhuber, T. Schroeder, Hematopoietic cytokines can instruct lineage choice. *Science* **325**, 217–218 (2009). Medline doi:10.1126/science.1171461

42. P. M. Lansdorp, W. Dragowska, H. Mayani, Ontogeny-related changes in proliferative potential of human hematopoietic cells. *J. Exp. Med.* **178**, 787–791 (1993). Medline doi:10.1084/jem.178.3.787

43. W. W. Pang, E. A. Price, D. Sahoo, I. Beerman, W. J. Maloney, D. J. Rossi, S. L. Schrier, I. L. Weissman, Human bone marrow hematopoietic stem cells are increased in frequency and myeloid-biased with age. *Proc. Natl. Acad. Sci. U.S.A.* **108**, 20012–20017 (2011). Medline

44. F. Notta, S. Doulatov, J. E. Dick, Engraftment of human hematopoietic stem cells is more efficient in female NOD/SCID/IL-2Rgc-null recipients. *Blood* **115**, 3704–3707 (2010). Medline doi:10.1182/blood-2009-10-249326

SUPPLEMENTARY FIGURE AND TABLE LEGENDS

Figure S1: Detailed gating scheme of HSC and progenitor cell subsets from FL, CB and BM used in this study.
(A-C) Representative plots of CD34+ selected FL (A), CB (B) and BM (C) subjected to an 11 parameter flow sorting scheme are shown. Dead cells were excluded using propidium iodide (not shown). Cells were subsequently subdivided into CD34+CD38- and CD34+CD38+ compartments (Panel 1). Within the CD34+CD38- compartment, CD71 and BAH1 expression defined MPP F2 and F3 (Panel 2). Cells lacking CD71 and BAH1 expression in the CD34+CD38- compartment (double negative gate in Panel 2) were further gated for HSCs and MPPs (MPP F1) on the basis on Thy1 and CD49f (Panels 3-5). Within the CD34+CD38+ compartment, CD10– cells (to exclude lymphoid cells – Panel 6) were fractionated with FLT3 and CD45RA to define classical CMPs, GMPs and MEPs (Panels 7). CMPs and MEPs were further subfractionated according to CD71 and BAH-1 expression (Panels 8,10: F1, F2, F3). CD19 expression was used to exclude CD45RA+ B-cells from the GMP population (Panels 9). Blue arrows indicate the gating hierarchy used during sorting.

Figure S2: Assessment of the markers used to establish subpopulations within MPP, CMPs and MEPs. (A) Thy1+CD45RA+ (left) cells from CD34+CD38- (shown in fig. S1) that are enriched for HSCs were analyzed for CD71 (middle) and BAH1 (right) expression. A representative flow plot from BM is shown. **(B)** Analysis of CD45RA and CD71 expression in the CD34+CD38- compartment demonstrates that these markers are expressed in a mutually exclusive manner. Representative plot from FL is shown. **(C)** Within FL CD34+CD38+ compartment, CD7+ cells (left) express high levels of myeloid differentiation marker, FLT3 (right – blue). FLT3 expression in CD10+ lymphoid cells was used as a negative control (right - red). Black arrows show gating scheme. **(D)** Backgating of CD71+BAH1- (F2s) and CD71+BAH1+ (F3s) fractions against classical CMP, MEP and GMP populations.

Figure S3: Methylcellulose (MC) and Megacult colony assays for CD34+ subsets from FL, CB and BM used in this study. (A) For each colony assay 100 sorted cells were plated in duplicates. Cloning efficiency per 100 plated cells for each colony type is shown on the y-axis. Colonies from MC were scored for colony forming units (CFU) 14 days after plating. **(B)** High proliferative potential (CFU-HPP) colonies were scored as colonies that were >1000 cells. **(C)** Megacult colonies (CFU-Mk) were assessed 10 days after plating using GPIIb/IIa specific antibody. **(D)** CFU-Mk were segregated according to size established in MegaCult manual (Stem cell Technologies). Residual colonies (3 – 20 cells) that did not pass our threshold in the analysis are shown in fig. S4D. Bars indicate mean at least three biological replicates ± s.e.m.

Figure S4: Assessment of colony size from MPP, CMPs and MEPs subsets in FL and BM. (A) To determine the average colony size from each population assayed in the MC assay from fig. S3A, duplicate culture plates were harvested and cells counted using ViCell XR. Cell counts were subsequently divided by the total number of CFU to obtain the average colony size. **(B)** Fold difference in colony size from **A** between FL and BM. **(C)** Representative flow cytometry analysis of Er colonies from FL MEP F3. To distinguish Er colonies from My colonies from FL populations, randomly selected colonies were harvested and analyzed for GlyA expression by flow cytometry. In FL, some Er colonies appeared to morphologically resemble myeloid colonies

likely due to reduced hemoglobinization. Bars indicate mean of at least three biological replicates ± s.e.m.

Figure S5: Lineage analysis of single cell clones from HSC, MPP F1, CMP F1 and GMP from FL, CB and BM. (A) Lineage potential and colony distribution of single cells clones from HSC and GMP subsets. Examples of various clone types (Mix, My, Mk, E/Mk/E) are shown in Fig. 3A. **(B-C)** Distribution of double (double: Er/My or Mk/My) and triple mixed (triple: Er/My/Mk) colonies from HSC/MPP F1 (B) and CMP F1 (C).

Figure S6: Kinetics of engraftment of CB HSC subset into NSG mice. (A) Relative proliferative capacity of HSC and MPP/CMP/MEP populations in FL (left) and BM (right) subsets. The size of the circle represents the proliferative potential from colony assays. The lineage potential of each subset is depicted as a pie graph in each circle. **(B)** Few hundred freshly sorted CD49f+ HSCs from CB were transplanted into large cohort of female NSG recipients. Recipients (~3-4/timepoint) were sacrificed at multiple timepoints (2, 4, 8, 16, 24 wk) after transplant and analyzed for all major human cell lineages in the injected femur (left) and non-injected bones (right) using flow cytometry. Total human cell engraftment (CD45+) and lineage assessment (B-lymphoid - CD19; total myeloid - CD33+; granulocyte – CD15+CD14-; monocyte – CD14+; erythroid – GlyA+CD71+) is represented both as a percentage (column 1) and in absolute numbers (column 2). **(C)** Temporal analyses of total human cell engraftment (CD45+, left) and human platelets (CD41+CD42b+) from HSC. **(D)** Human platelets in the peripheral blood of NSG mice were detected in rare recipients transplanted with CB MPP F1 and MPP2/3. This analysis was performed 2 weeks after transplant. A negative control (no human cells transplanted) and positive control (HSC) are shown as a comparison. **(E)** Total Er (GlyA+, top) and human cell engraftment (CD45+, bottom) from cell subsets from injected femur and non-injected bones two weeks after transplant. Bars indicate mean ± standard error from two independent experiments (n = 3 – 21 mice).

Figure S7: Gene expression analysis of HSC and MPP, CMP, MEP subsets. (A) CB subsets in biological duplicates were sorted and subjected to SMARTseq protocol for low input RNA sequencing using Illumina HiSeq platform. Fastq files aligned with STAR and gene expression analysis was performed using cufflinks package. Transcritp levels (FPKM) of lineage factors associated My (*MPO*, *CSF2RA*), Mk (*CD41* and *CD42b*), Er (*GATA1*, *EPOR*). Housekeeping genes, *PGK1* and *GAPDH* were used as a control. FPKM – fragments per kilobase of exon per million fragments mapped). **(B)** Unsupervised clustering (i) and principal component analysis (ii) of all CB subsets. **(C)** GO analysis using DAVID of differentially expressed genes from Er subsets (MPP F2/3, CMP F2/3, MEP F2/3). These differentially expressed genes were highly enriched in cell cycle, DNA replication and metabolic processes. **(D)** Additional populations for single cell fluidigm analysis from Fig. 5A (FL MPP F3, FL CMP F3 and BM MPP F1).

Table S1: List of flow sorted subsets used in this study. Complete phenotype and their percentage (± s.e.m) within the CD34+ fraction are shown.

Figure S1

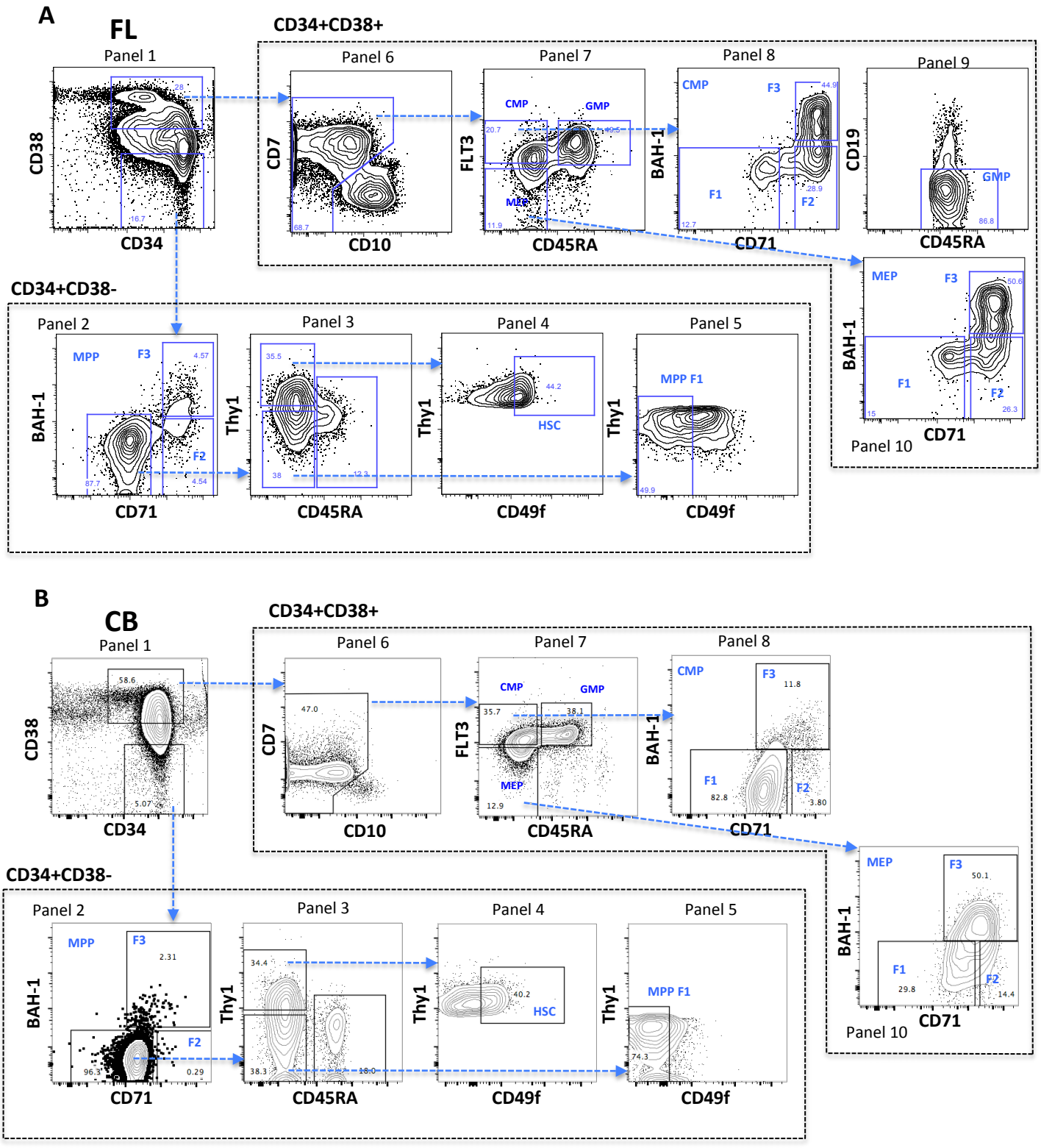
A
FL
CD34+CD38+
CD34+CD38-
Panel 1
CD38
CD34
Panel 6
CD7
CD10
Panel 7
FLT3
CD45RA
CMP
GMP
MEP
Panel 8
BAH-1
CD71
F1
F2
F3
Panel 9
CD19
CD45RA
GMP
Panel 10
MEP
Panel 2
MPP
Panel 3
Thy1
CD45RA
Panel 4
HSC
CD49f
Panel 5
MPP F1
B
CB

Figure S1

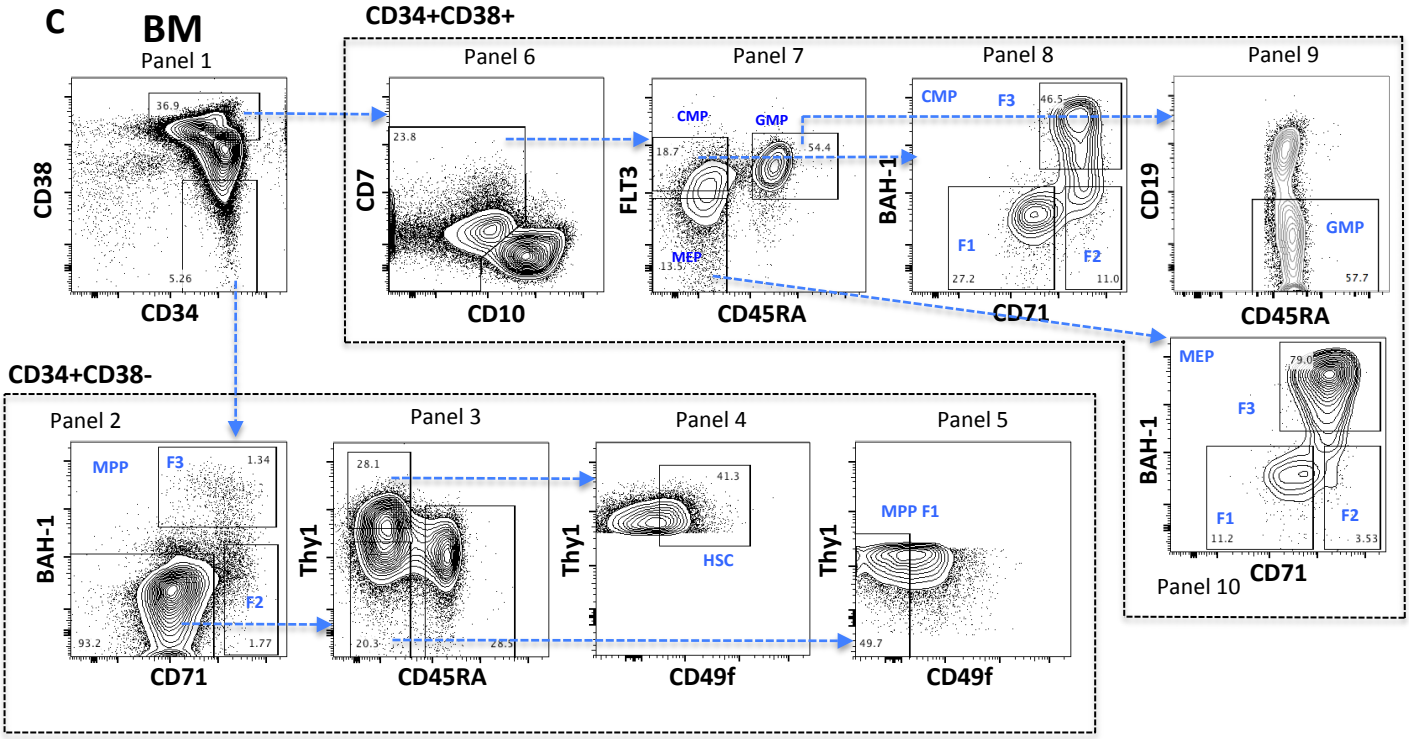
C
BM
Panel 1
CD38
CD34
36.9
5.26
CD34+CD38+
Panel 6
CD7
CD10
23.8
Panel 7
FLT3
CD45RA
CMP
GMP
MEP
18.7
54.4
13.5
Panel 8
BAH-1
CD71
CMP
F3
F1
F2
46.5
27.2
11.0
Panel 9
CD19
CD45RA
GMP
57.7
CD34+CD38-
Panel 2
BAH-1
CD71
MPP
F3
F2
1.34
93.2
1.77
Panel 3
Thy1
CD45RA
28.1
20.3
28.5
Panel 4
Thy1
CD49f
41.3
HSC
Panel 5
Thy1
CD49f
MPP F1
49.7
Panel 10
BAH-1
CD71
MEP
F3
F1
F2
79.0
11.2
3.53

Figure S2

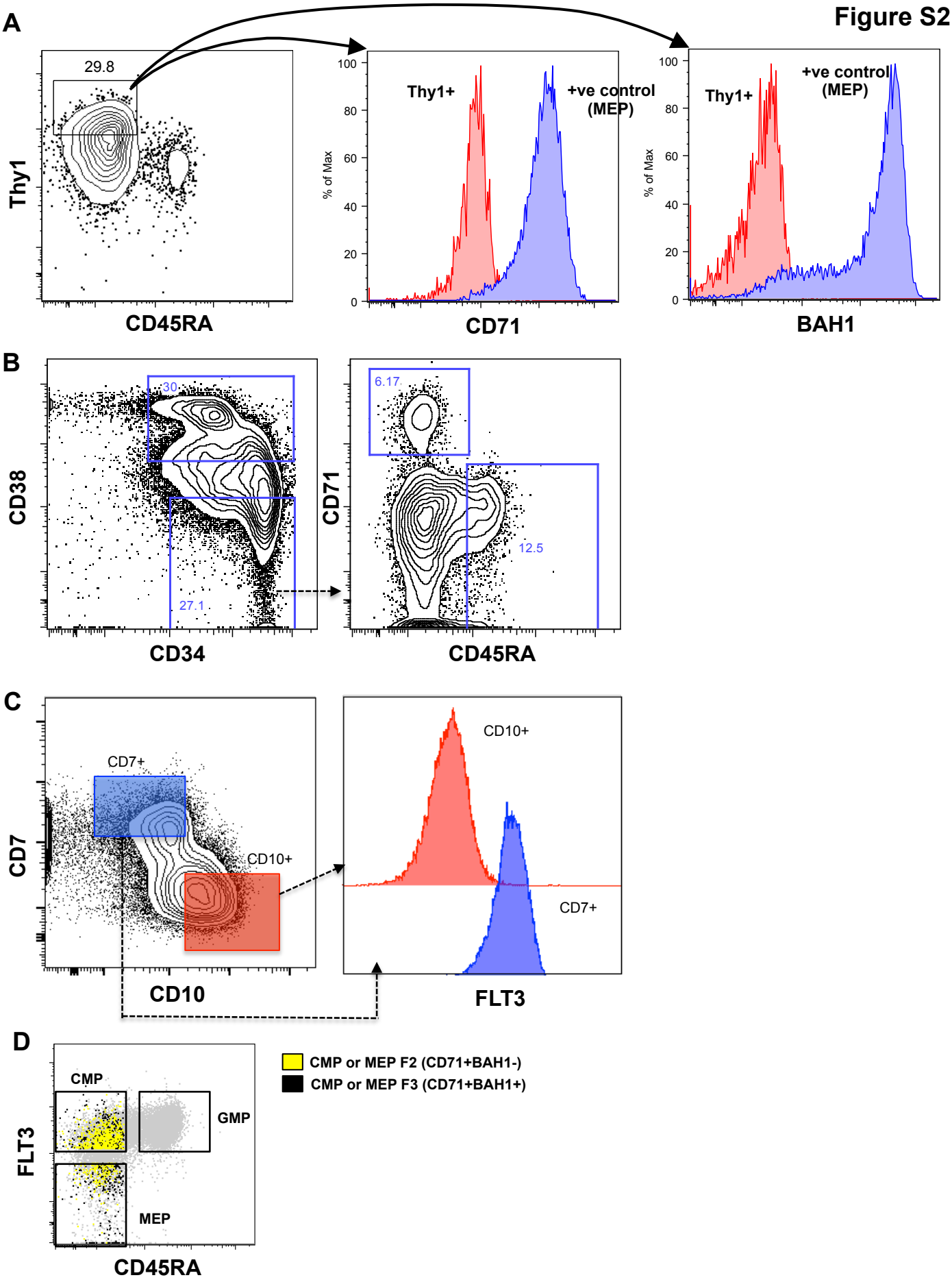
A
29.8
Thy1
CD45RA
Thy1+
+ve control
(MEP)
% of Max
CD71
BAH1
B
30
27.1
CD38
CD34
6.17
12.5
CD71
CD45RA
C
CD7+
CD10+
CD7
CD10
CD10+
CD7+
FLT3
D
CMP
GMP
MEP
FLT3
CD45RA
CMP or MEP F2 (CD71+BAH1-)
CMP or MEP F3 (CD71+BAH1+)

Figure S3

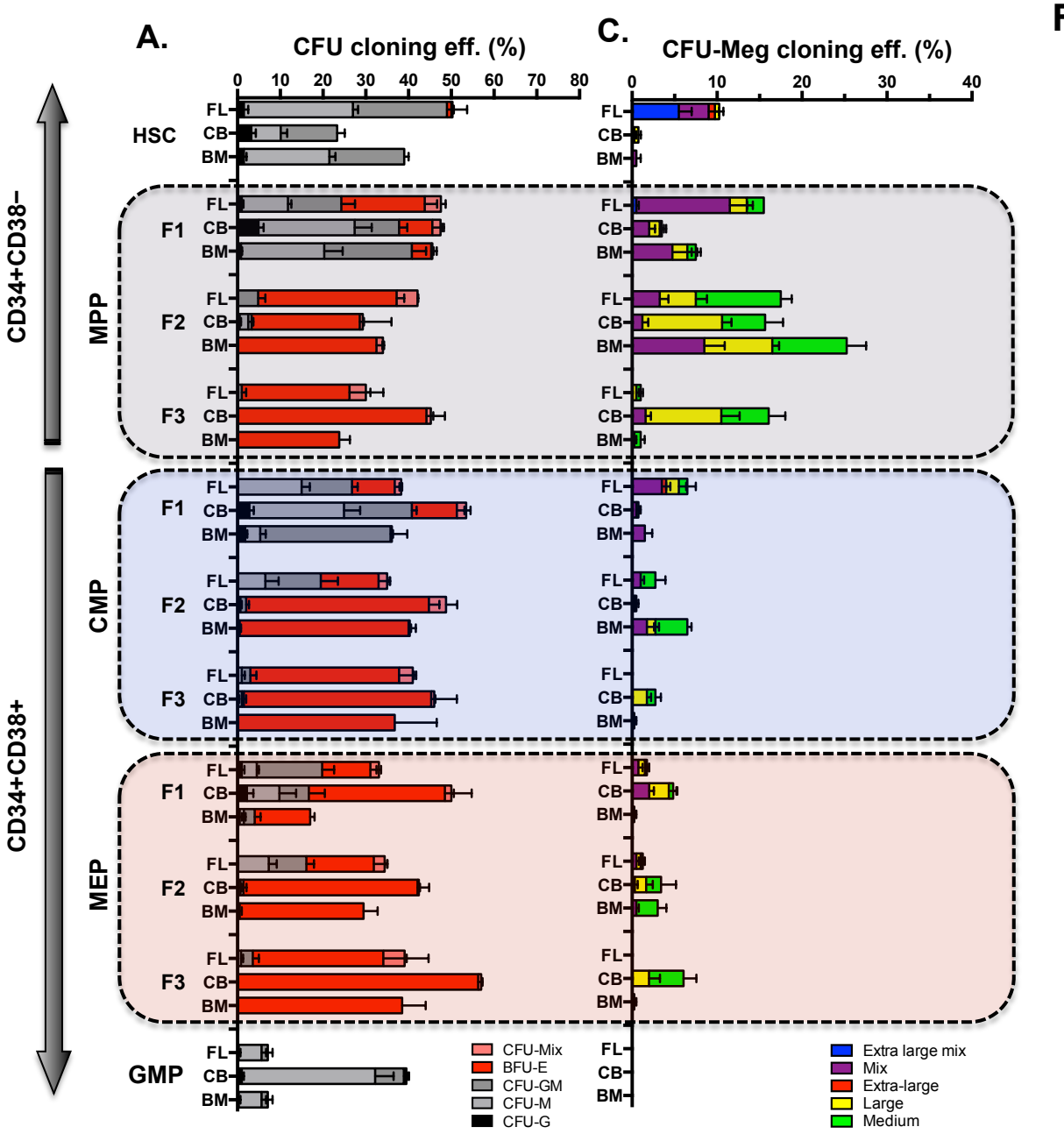
A.
CFU cloning eff. (%)
0 10 20 30 40 50 60 70 80
C.
CFU-Meg cloning eff. (%)
0 10 20 30 40
CD34+CD38−
CD34+CD38+
HSC
MPP
CMP
MEP
GMP
F1
F2
F3
FL
CB
BM
CFU-Mix
BFU-E
CFU-GM
CFU-M
CFU-G
Extra large mix
Mix
Extra-large
Large
Medium

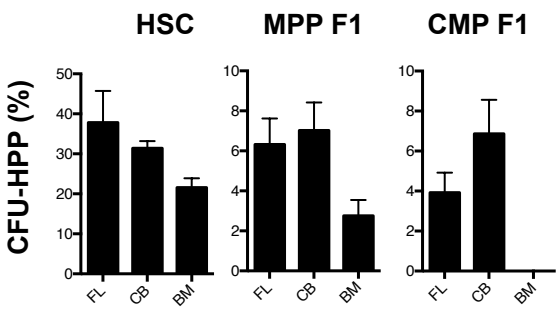
B.
HSC
MPP F1
CMP F1
CFU-HPP (%)
FL
CB
BM

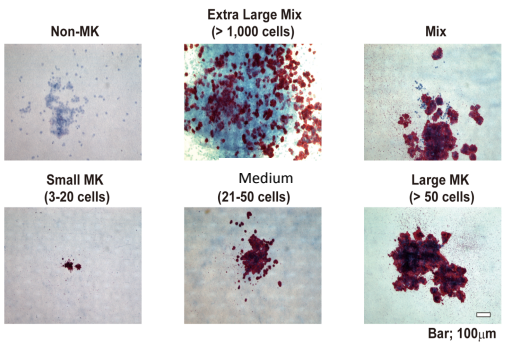
D.
Non-MK
Extra Large Mix
(> 1,000 cells)
Mix
Small MK
(3-20 cells)
Medium
(21-50 cells)
Large MK
(> 50 cells)
Bar; 100μm

Figure S4

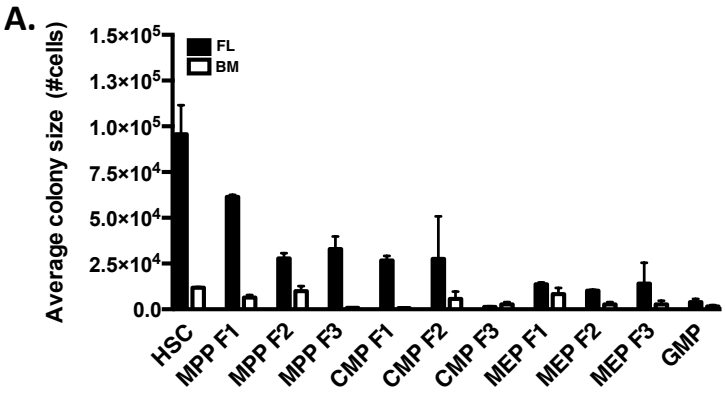
A.
Average colony size (#cells)
1.5×10^5
1.3×10^5
1.0×10^5
7.5×10^4
5.0×10^4
2.5×10^4
0.0
FL
BM
HSC
MPP F1
MPP F2
MPP F3
CMP F1
CMP F2
CMP F3
MEP F1
MEP F2
MEP F3
GMP

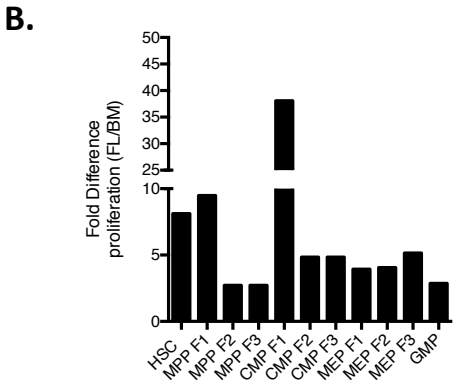
B.
Fold Difference proliferation (FL/BM)
50
45
40
35
30
25
10
5
0
HSC
MPP F1
MPP F2
MPP F3
CMP F1
CMP F2
CMP F3
MEP F1
MEP F2
MEP F3
GMP

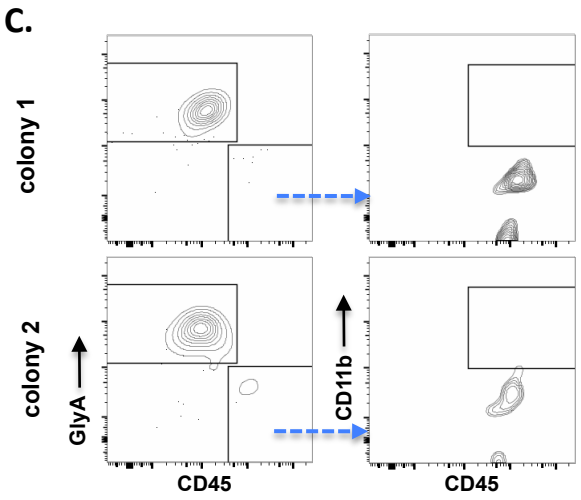
C.
colony 1
colony 2
GlyA
CD11b
CD45
CD45

Figure S5

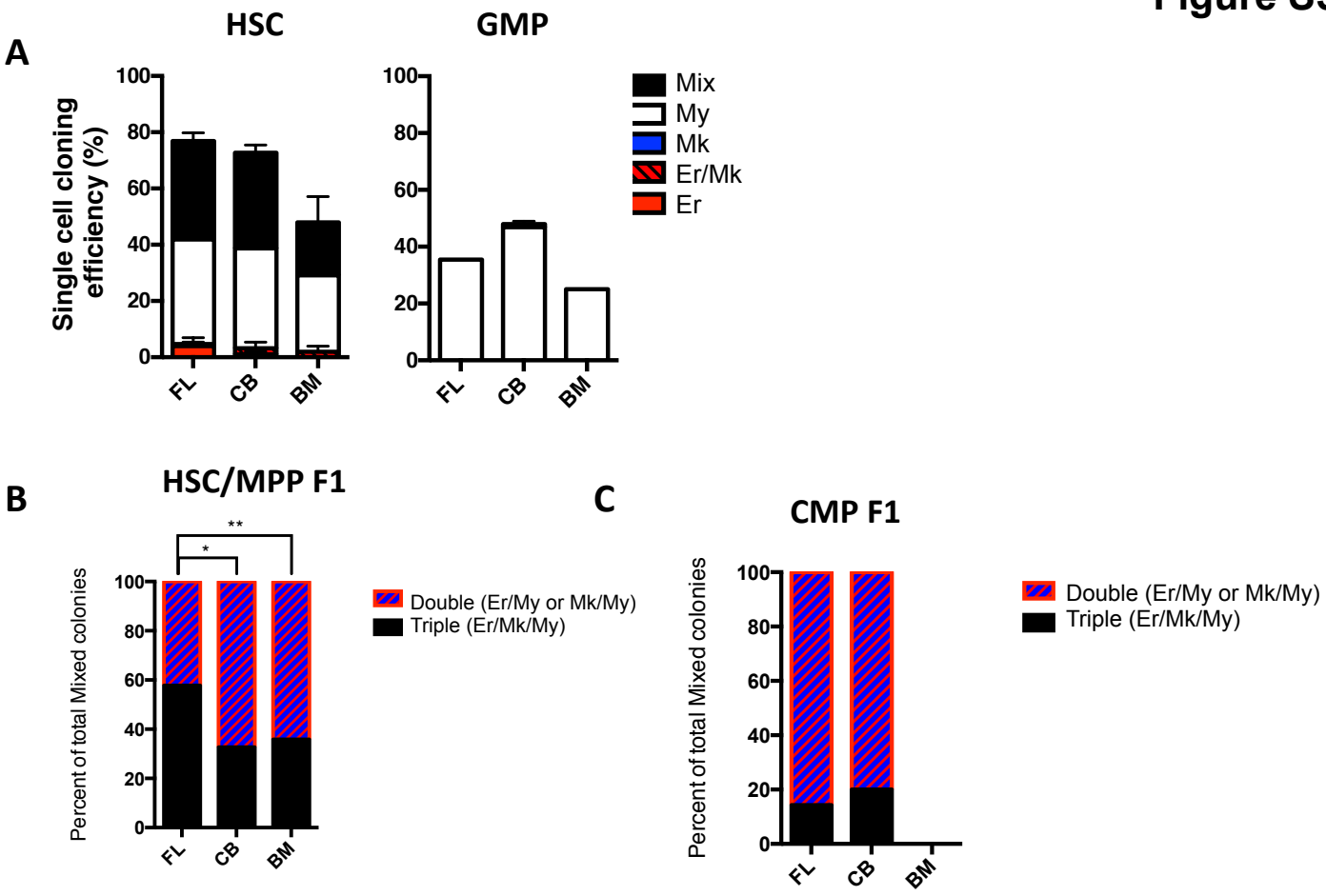
A
HSC
GMP
Single cell cloning efficiency (%)
100
80
60
40
20
0
FL
CB
BM
Mix
My
Mk
Er/Mk
Er
B
HSC/MPP F1
Percent of total Mixed colonies
**
*
Double (Er/My or Mk/My)
Triple (Er/Mk/My)
C
CMP F1
Percent of total Mixed colonies
Double (Er/My or Mk/My)
Triple (Er/Mk/My)

Figure S6

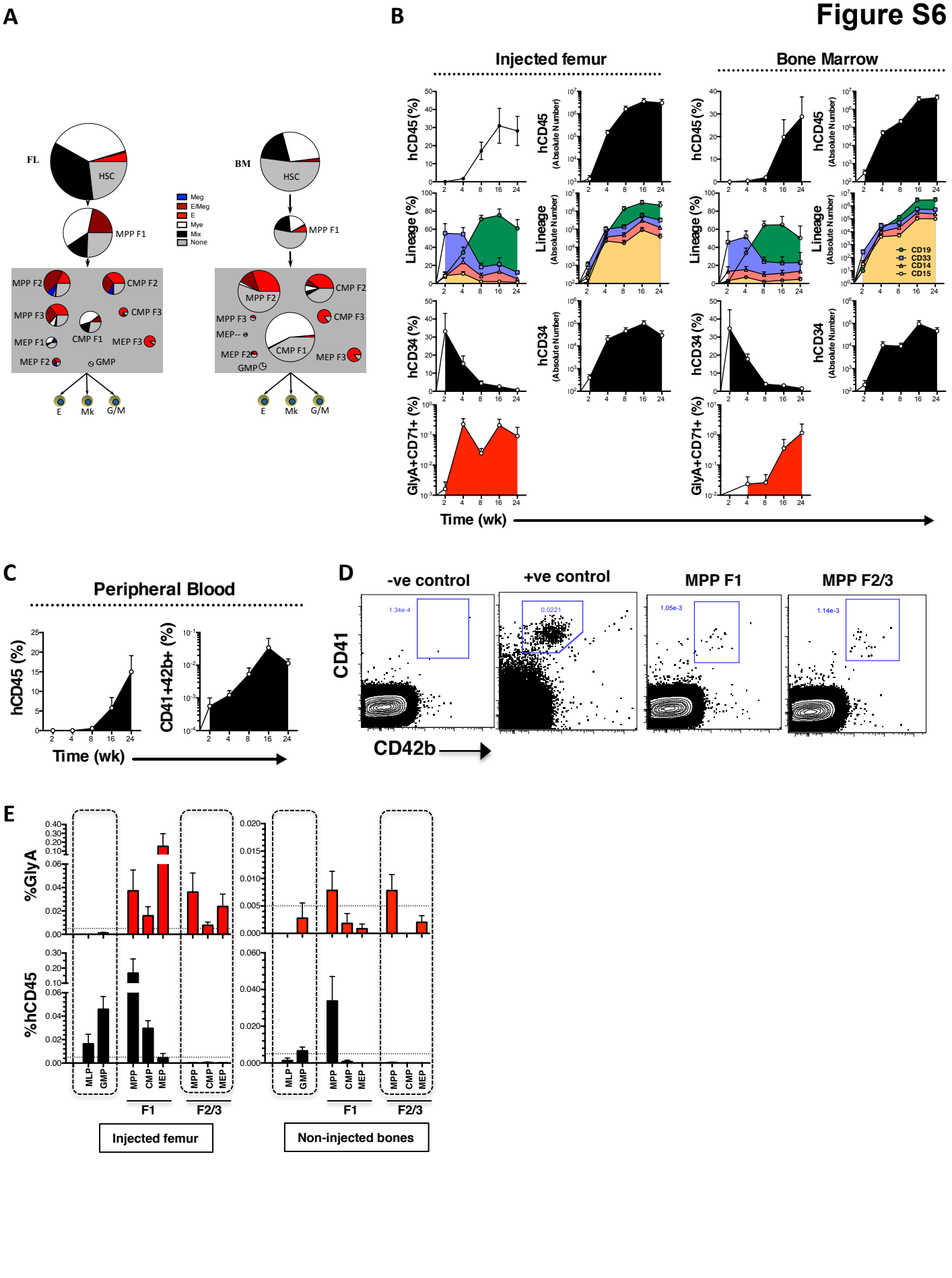
A
FL
HSC
MPP F1
MPP F2
CMP F2
MPP F3
CMP F3
CMP F1
MEP F1
MEP F3
MEP F2
GMP
E
Mk
G/M
BM
HSC
MPP F1
MPP F2
CMP F2
MPP F3
CMP F3
MEP--
CMP F1
MEP F2
MEP F3
GMP
E
Mk
G/M
Meg
E/Meg
E
Mye
Mix
None
B
Injected femur
Bone Marrow
hCD45 (%)
hCD45 (Absolute Number)
Lineage (%)
Lineage (Absolute Number)
CD19
CD33
CD14
CD15
hCD34 (%)
hCD34 (Absolute Number)
GlyA+CD71+ (%)
Time (wk)
C
Peripheral Blood
hCD45 (%)
CD41+42b+ (%)
Time (wk)
D
-ve control
+ve control
MPP F1
MPP F2/3
CD41
CD42b
1.34e-4
0.0221
1.05e-3
1.14e-3
E
%GlyA
%hCD45
MLP
GMP
MPP
CMP
MEP
F1
F2/3
Injected femur
Non-injected bones

Figure S7

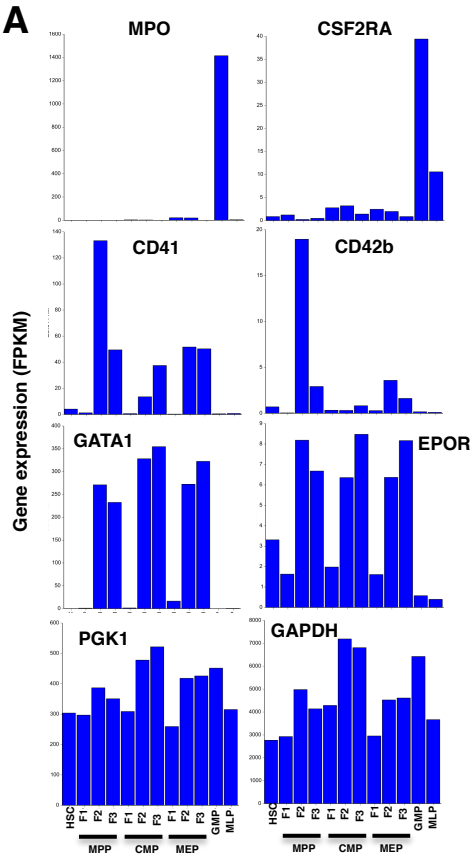

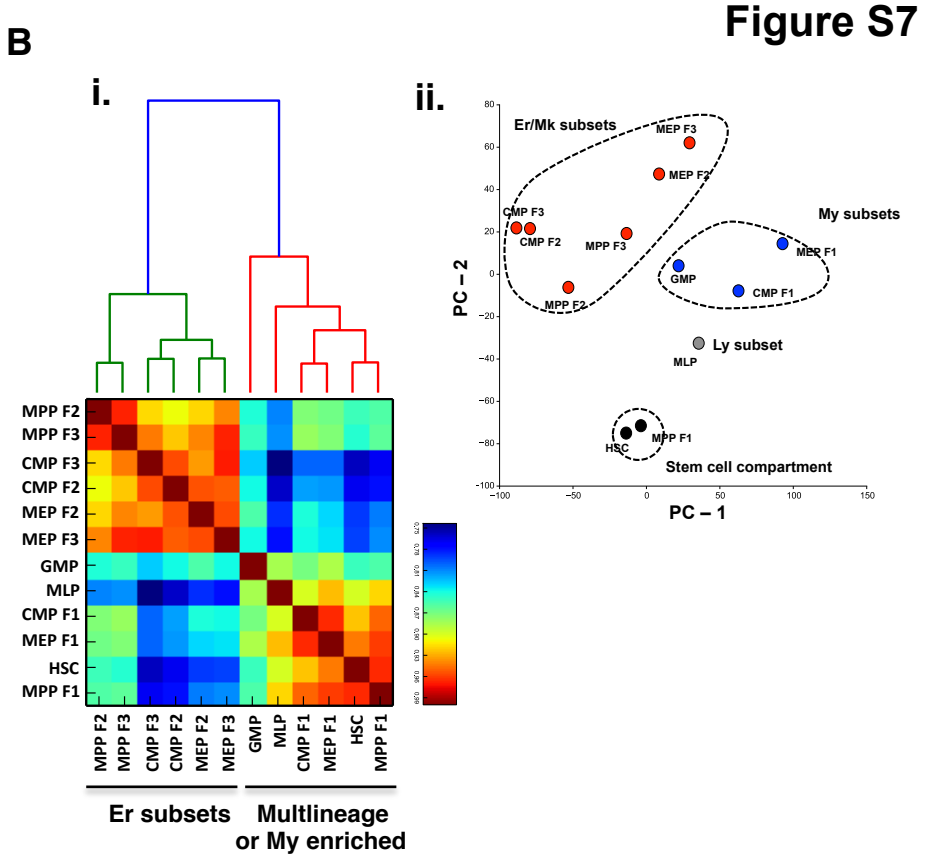

C

	Category	Term	No. of genes	PValue	FDR
1	BP	cell cycle	37	7.39E-10	1.24E-06
2	BP	DNA replication	17	2.16E-08	3.62E-05
3	BP	DNA metabolic process	25	4.57E-07	7.65E-04
4	BP	mitosis	16	9.32E-07	0.00155893
5	BP	nuclear division	16	9.32E-07	0.00155893
6	BP	nucleosome organization	11	1.11E-06	0.00185417
7	BP	M phase of mitotic cell cycle	16	1.18E-06	0.00197381
8	BP	DNA packaging	12	1.24E-06	0.00207334
9	BP	organelle fission	16	1.56E-06	0.00260221
10	BP	M phase	19	1.88E-06	0.00314038

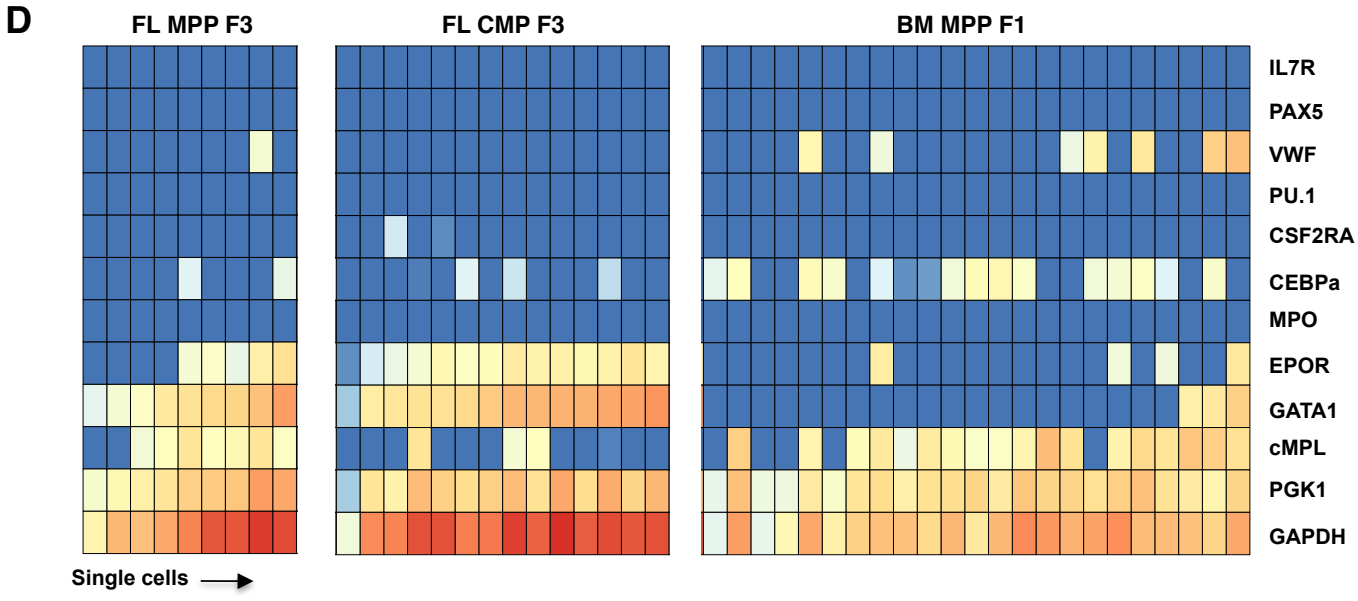

Table S1

Population	Cell Phenotype	FL (%)	CB (%)	BM (%)	FL / BM	CB / BM
HSC	CD34+38−/lo45RA−Thy1+49f+71−BAH1−	5.43 (±0.67)	1.52 (±0.21)	1.19 (±0.18)	4.6	1.3
MPP F1	CD34+38−/lo45RA−Thy1−49f−71−BAH1−	3.92 (±0.65)	2.05 (±0.29)	0.81 (±0.21)	4.8	2.5
MPP F2	CD34+38−/lo45RA−Thy1−71+BAH1−	1.23 (±0.33)	0.29 (±0.07)	0.01 (±0.01)	91.1	5.1
MPP F3	CD34+38−/lo45RA−Thy1−71+BAH1+	0.55 (±0.21)	0.20 (±0.04)	0.01 (±0.00)	41.8	15.1
CMP FI	CD34+38+10−45RA−Flt3+71−BAH1−	0.91 (±0.24)	21.94 (±3.66)	6.38 (±1.17)	-7.0	3.4
CMP F2	CD34+38+10−45RA−Flt3+71+BAH1−	1.31 (±0.44)	0.78 (±0.25)	1.28 (±0.51)	1.0	-1.6
CMP F3	CD34+38+10−45RA−Flt3+71+BAH1+	1.85 (±0.35)	1.80 (±0.38)	1.64 (±0.74)	1.1	1.1
MEP F1	CD34+38+10−45RA−Flt3−71−BAH1−	0.42 (±0.14)	2.26 (±0.34)	1.93 (±0.52)	-4.6	1.2
MEP F2	CD34+38+10−45RA−Flt3−71+BAH1−	0.79 (±0.33)	1.43 (±0.38)	0.88 (±0.24)	0.9	1.6
MEP F3	CD34+38+10−45RA−Flt3−71+BAH1+	1.11 (±0.20)	4.28 (±0.98)	4.05 (±0.63)	-3.6	1.1
GMP 7+	CD34+38+10−45RA+Flt3+ CD7+	8.37 (±0.64)	1.81 (±0.18)	0.59 (±0.07)	14.2	3.1
GMP 7−	CD34+38+10−45RA+Flt3+CD7−	0.34 (±0.25)	8.58 (±2.26)	20.17 (±1.50)	-60.0	-2.4
Lymphoid	CD34+CD38+10+	13.09 (±5.08)	4.96 (±1.42)	27.15 (±2.98)	-2.1	-5.5